Supporting Information

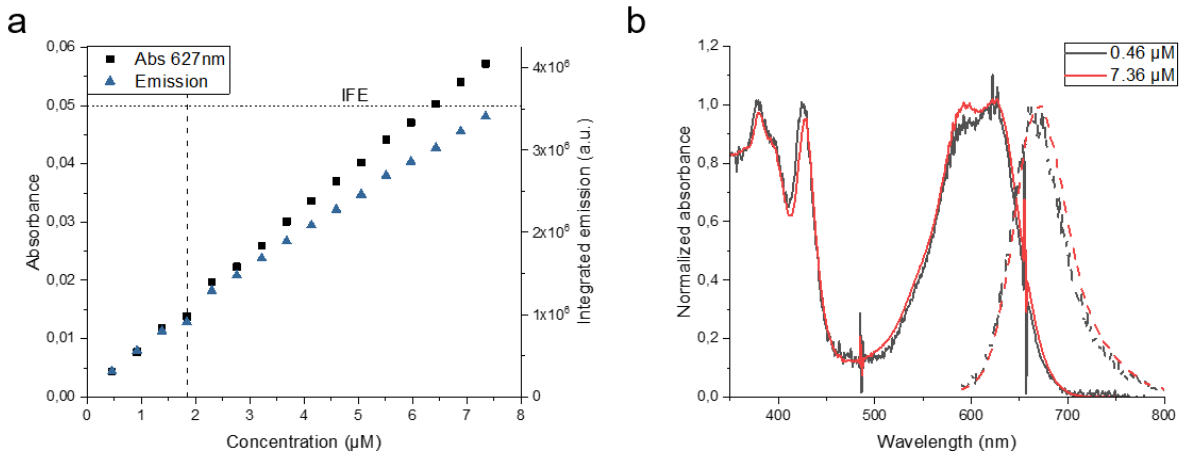

Figure S1: (a) The absorbance (at 627 nm) and integrated emission (excitation at 580 nm) of **BDATA-M2** plotted as functions of concentration of the dye. The vertical dashed line indicates the concentration at which the gradients of the absorbance and emission diverge, indicating the effect of aggregation. The horizontal dashed line indicates the absorbance (0.05) at which the inner filter effect would cause the absorbance and emission gradients to diverge. (b) Normalised absorbance (solid) and emission (dashed, excitation at 580 nm) spectra of **BDATA-M2** at low (black) and high (red) concentration of dye. At high concentration the shoulder of the absorbance spectrum becomes a more defined peak, showing the impact of aggregation.

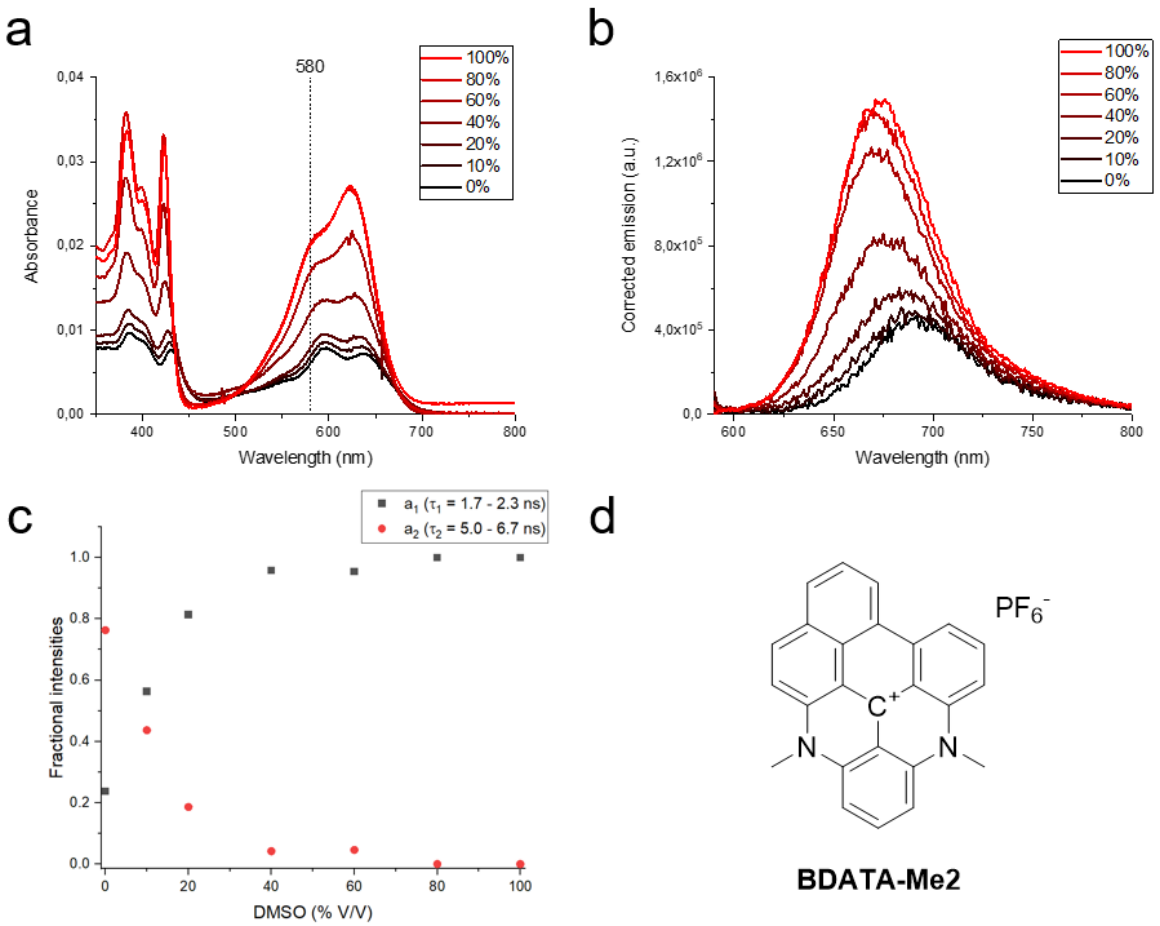

Figure S2: (a) Absorption spectra of **BDATA-Me2** in water/DMSO mixtures, with increasing concentration of DMSO (0-100% v/v). (b) Fluorescence emission spectra of **BDATA-Me2** in water/DMSO mixtures, with increasing concentration of DMSO (0-100% v/v). The changes in the spectra of a) and b) are consistent with DMSO being able to dissolve dye aggregates. Samples were excited at 580 nm and corrected for the absorbance. (c) The change in the amplitudes of fluorescence lifetime components of **BDATA-Me2** with increasing concentration of DMSO. Time-resolved fluorescence decays were fitted using biexponential analysis – the fractional intensities of the long (5.0-6.7 ns) and short (1.7-2.3 ns) components are displayed. (d) Structure of the parent chromophore used in these studies – **BDATA-Me2**.

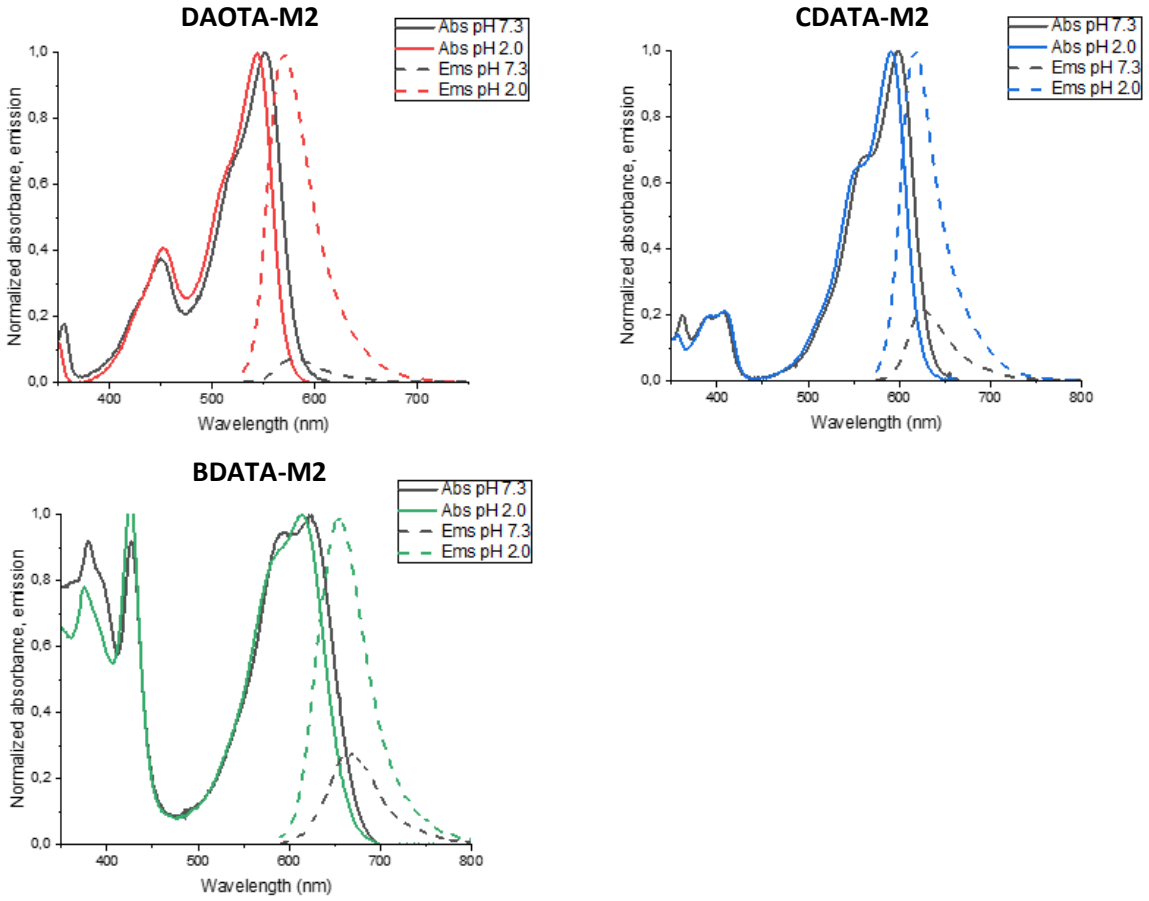

Figure S3: Absorbance (solid) and emission (dashed) spectra of **DAOTA-M2** (red), **CDATA-M2** (blue) and **BDATA-M2** (green) at physiological pH 7.3 and acidic pH 2.0. The absorbance and emission spectra at pH 2 were normalised, while the spectra at pH 7.3 was scaled in relation to pH 2. A change in absorbance and increased emission were observed upon protonation of the morpholino groups appended to the fluorophores. These changes are due to reduced aggregation (for **BDATA-M2**) and to the reduced PET quenching (for **DAOTA-M2**, **CDATA-M2** and possibly a small contribution for **BDATA-M2**). Further acidification at pH 2.0 and basification at pH 7.3 did not alter the spectra further for any of the probes.

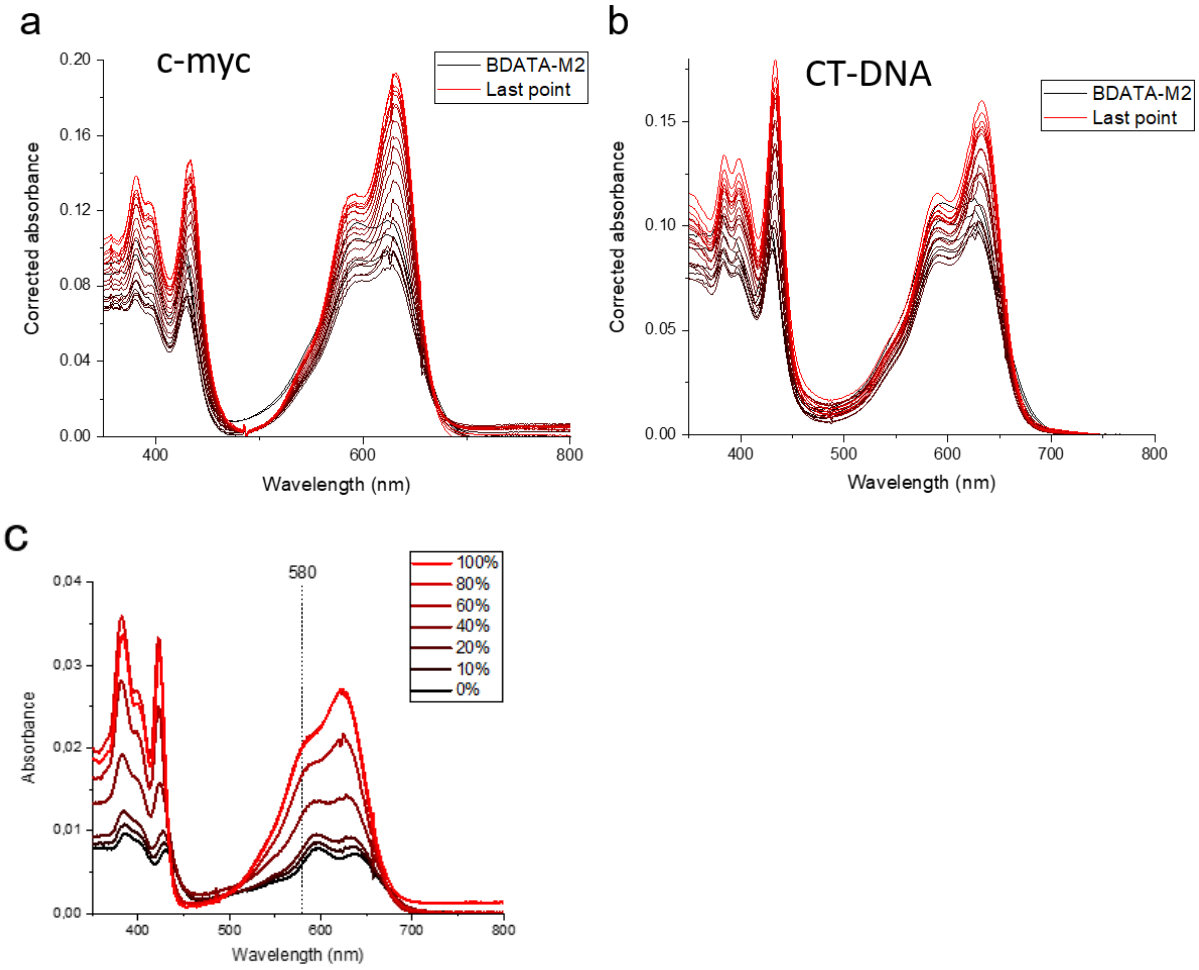

Figure S4: The change in absorbance spectra of **BDATA-M2** upon the addition of the increasing concentrations of G4 (c-myc, a) and non-G4 (CT-DNA, b) oligonucleotides, compared to the changes in **BDATA-Me2** absorbance upon addition of DMSO (c). For top figures, **BDATA-M2** only spectra are in black, with increasing DNA concentration indicated by increasing intensity of red colour. Increasing disaggregation of the dye is evidenced by the increase in the relative intensity of the peak at longer wavelength in all cases.

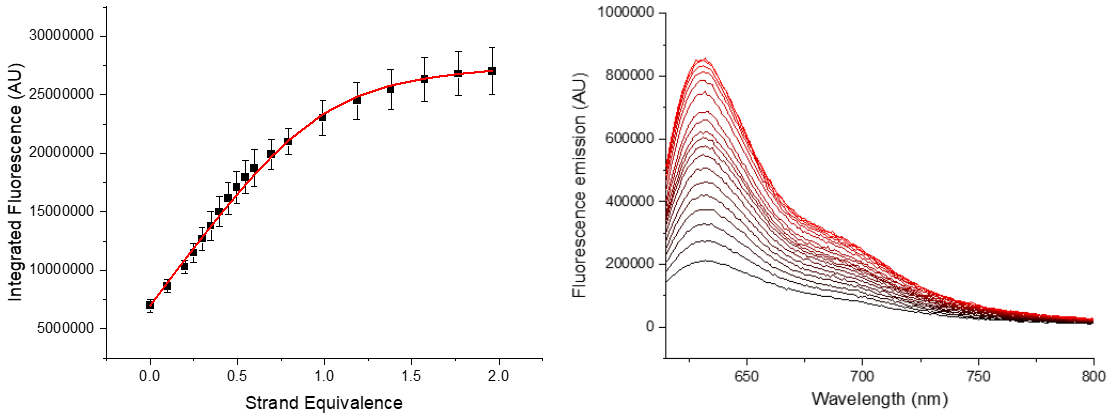

Figure S5: Emission titration of **CDATA-M2** with c-myc DNA oligonucleotide. Left panel shows the average integrated fluorescence of three repeats and standard deviation of those repeats. The red line shows the binding curve fit to the averages. Right panel shows the emission spectra from one representative titration. Lines are coloured from black to red to follow an increase in DNA concentration.

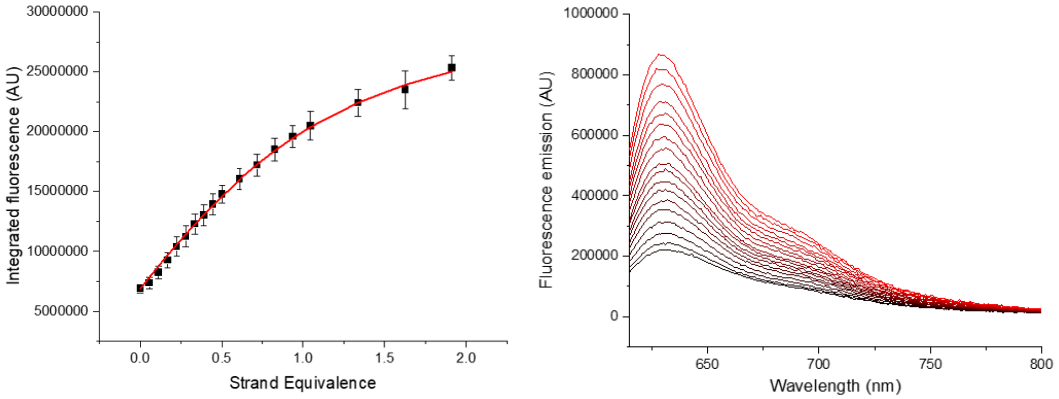

Figure S6: Emission titration of **CDATA-M2** with c-kit87up DNA oligonucleotide. Left panel shows the average integrated fluorescence of three repeats and standard deviation of those repeats. The red line shows the binding curve fit to the averages. Right panel shows the emission spectra from one representative titration. Lines are coloured from black to red to follow an increase in DNA concentration.

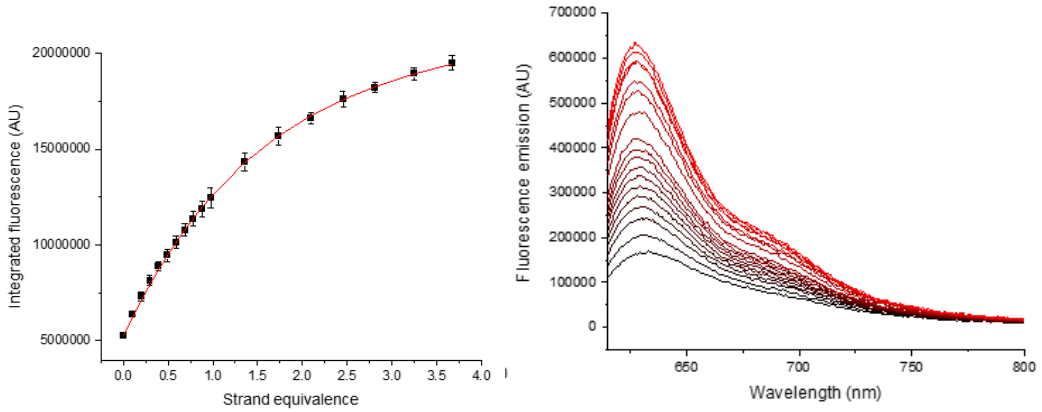

Figure S7: Emission titration of **CDATA-M2** with HRAS-1 DNA oligonucleotide. Left panel shows the average integrated fluorescence of three repeats and standard deviation of those repeats. The red

line shows the binding curve fit to the averages. Right panel shows the emission spectra from one representative titration. Lines are coloured from black to red to follow an increase in DNA concentration.

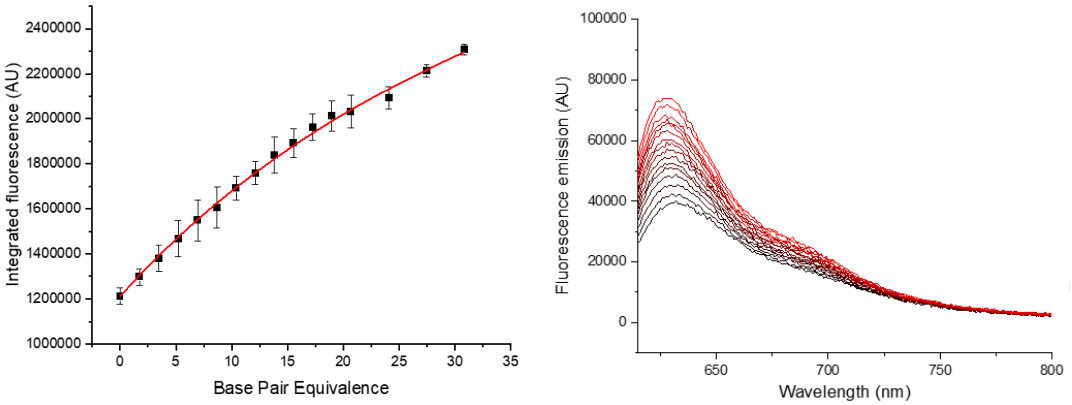

Figure S8: Emission titration of **CDATA-M2** with CT-DNA. Left panel shows the average integrated fluorescence of three repeats and standard deviation of those repeats. The red line shows the binding curve fit to the averages. Right panel shows the emission spectra from one representative titration. Lines are coloured from black to red to follow an increase in DNA concentration.

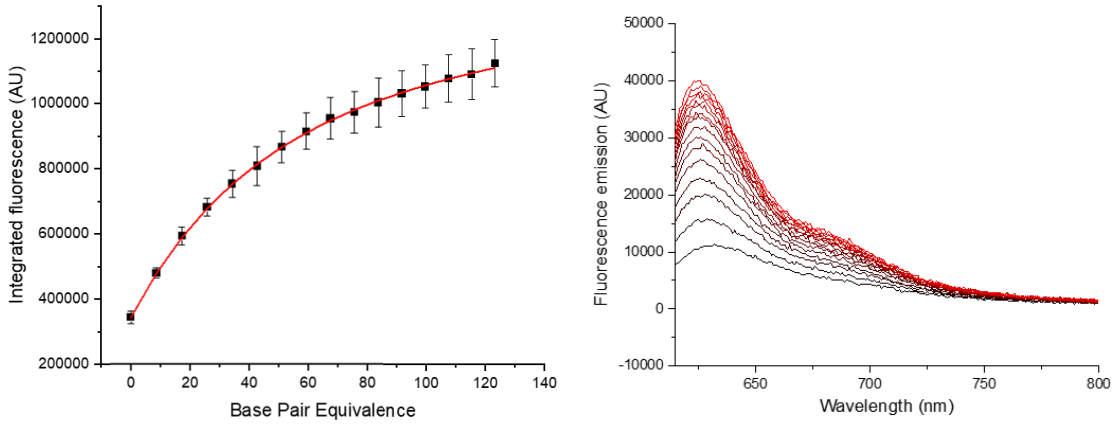

Figure S9: Emission titration of **CDATA-M2** with ds17 dsDNA oligonucleotide. Left panel shows the average integrated fluorescence of three repeats and standard deviation of those repeats. The red line shows the binding curve fit to the averages. Right panel shows the emission spectra from one representative titration. Lines are coloured from black to red to follow an increase in DNA concentration.

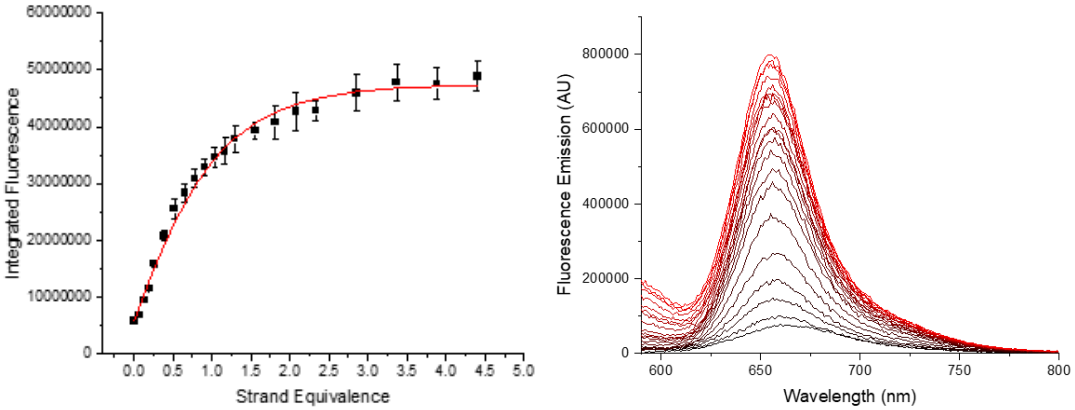

Figure S10: Emission titration of **BDATA-M2** with c-myc DNA oligonucleotide. Left panel shows the average integrated fluorescence of three repeats and standard deviation of those repeats. The red line shows the binding curve fit to the averages. Right panel shows the emission spectra from one representative titration. Lines are coloured from black to red to follow an increase in DNA concentration.

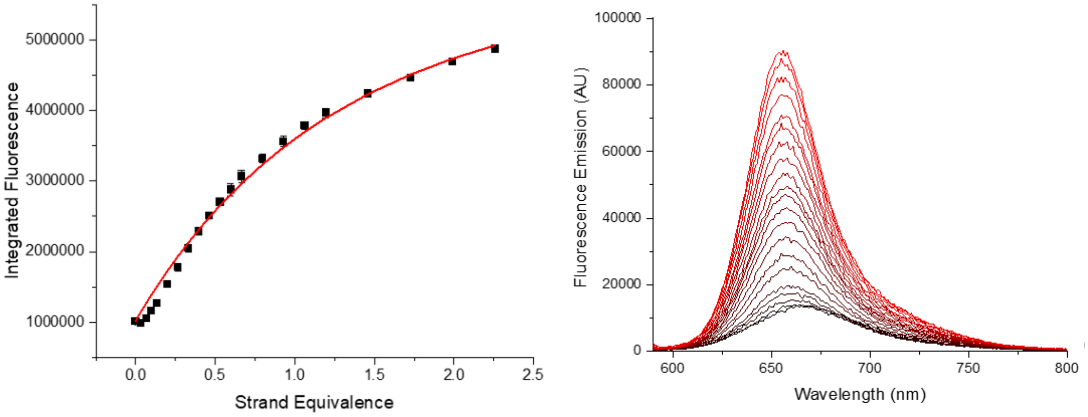

Figure S11: Emission titration of **BDATA-M2** with c-kit87up DNA oligonucleotide. Left panel shows the average integrated fluorescence of three repeats and standard deviation of those repeats. The red line shows the binding curve fit to the averages. Right panel shows the emission spectra from one representative titration. Lines are coloured from black to red to follow an increase in DNA concentration..

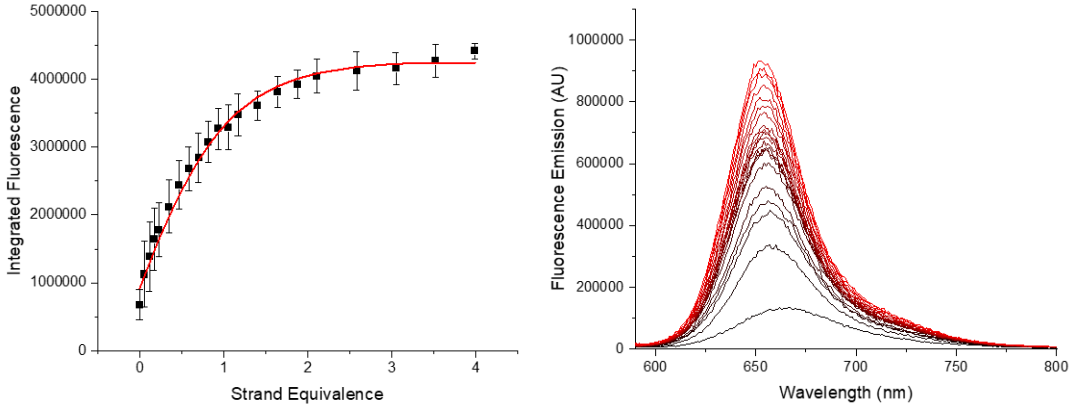

Figure S12: Emission titration of **BDATA-M2** with HRAS-1 DNA oligonucleotide. Left panel shows the average integrated fluorescence of three repeats and standard deviation of those repeats. The red line shows the binding curve fit to the averages. Right panel shows the emission spectra from one representative titration. Lines are coloured from black to red to follow an increase in DNA concentration.

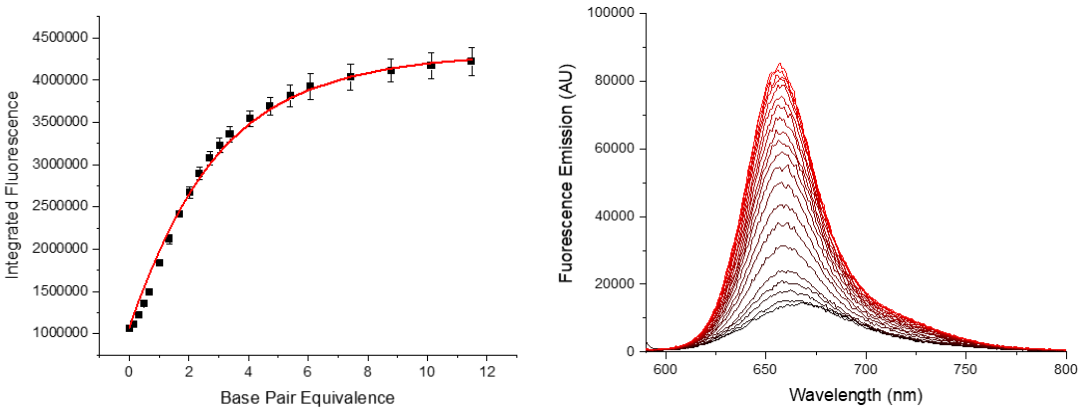

Figure S13: Emission titration of **BDATA-M2** with CT-DNA. Left panel shows the average integrated fluorescence of three repeats and standard deviation of those repeats. The red line shows the binding curve fit to the averages. Right panel shows the emission spectra from one representative titration. Lines are coloured from black to red to follow an increase in DNA concentration.

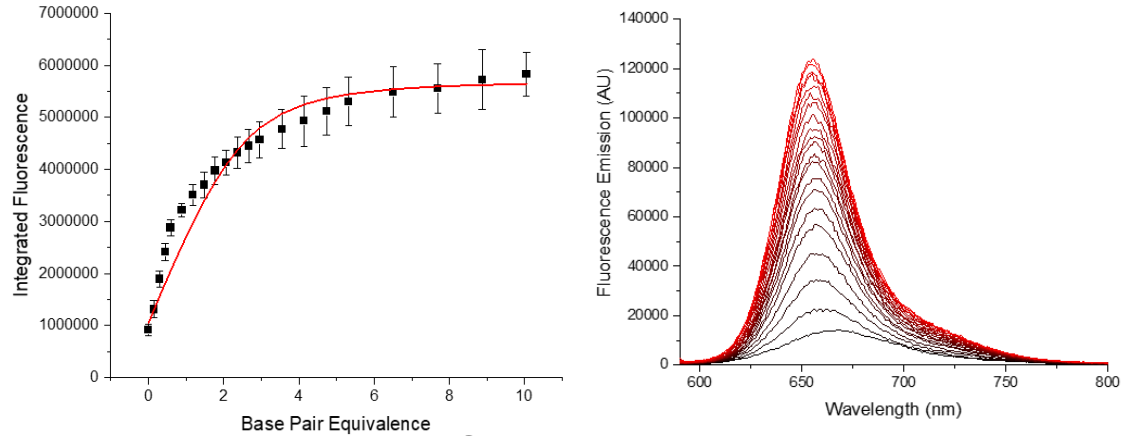

Figure S14: Emission titration of **BDATA-M2** with ds17 dsDNA oligonucleotide. Left panel shows the average integrated fluorescence of three repeats and standard deviation of those repeats. The red line shows the binding curve fit to the averages. Right panel shows the emission spectra from one representative titration. Lines are coloured from black to red to follow an increase in DNA concentration.

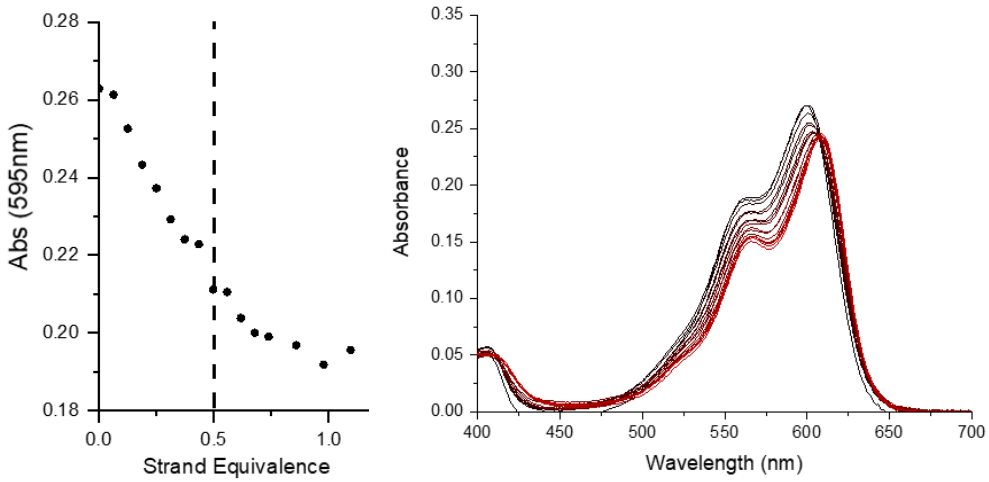

Figure S15: Absorption titration of **CDATA-M2** with c-myc DNA oligonucleotide. Left panel shows the absorbance at 595nm for a range of DNA strand equivalences, with the vertical dashed line indicating the stoichiometry of binding. Right panel shows the absorption spectra recorded during the titration. Lines are coloured from black to red to show increasing DNA concentration.

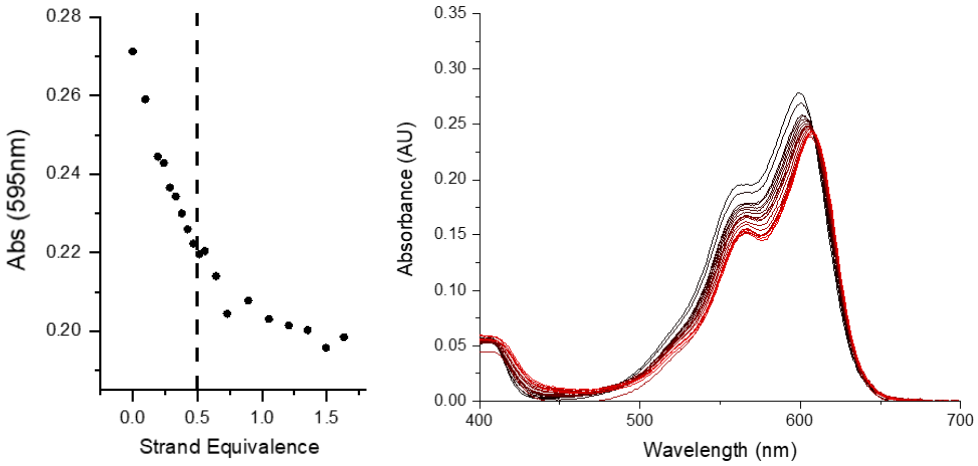

Figure S16: Absorption titration of **CDATA-M2** with c-kit87up DNA oligonucleotide. Left panel shows the absorbance at 595nm for a range of DNA strand equivalences, with the vertical dashed line indicating the stoichiometry of binding. Right panel shows the absorption spectra recorded during the titration. Lines are coloured from black to red to show increasing DNA concentration.

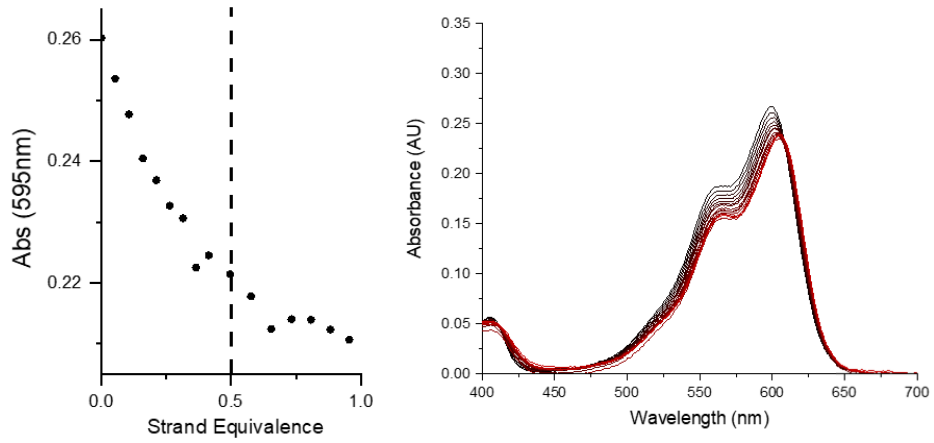

Figure S17: Absorption titration of **CDATA-M2** with HRAS-1 DNA oligonucleotide. Left panel shows the absorbance at 595nm for a range of DNA strand equivalences, with the vertical dashed line indicating the stoichiometry of binding. Right panel shows the absorption spectra recorded during the titration. Lines are coloured from black to red to show increasing DNA concentration.

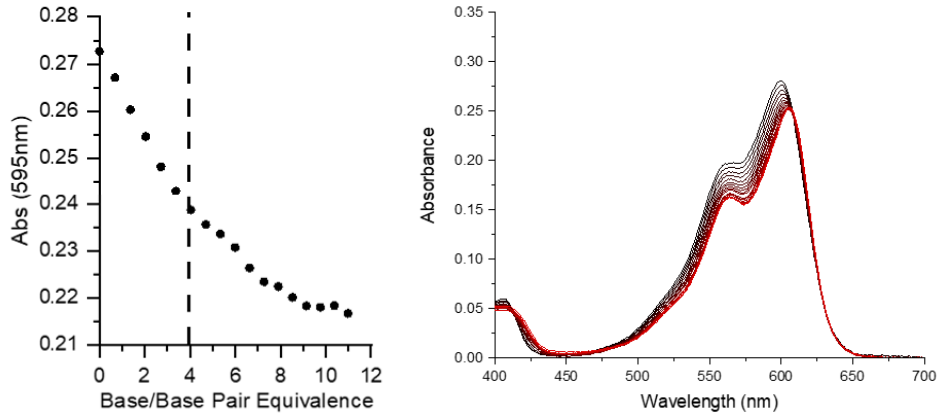

Figure S18: Absorption titration of **CDATA-M2** with CT-DNA. Left panel shows the absorbance at 595nm for a range of DNA strand equivalences, with the vertical dashed line indicating the stoichiometry of binding. Right panel shows the absorption spectra recorded during the titration. Lines are coloured from black to red to show increasing DNA concentration.

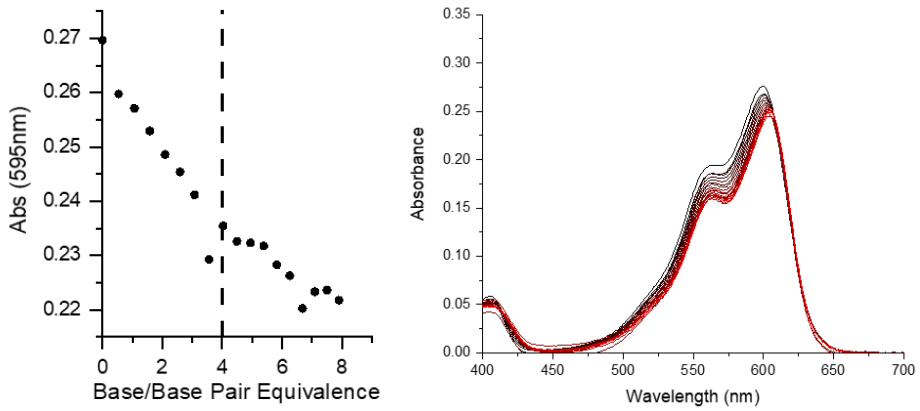

Figure S19: Absorption titration of **CDATA-M2** with ds17 dsDNA oligonucleotide. Left panel shows the absorbance at 595nm for a range of DNA strand equivalences, with the vertical dashed line indicating the stoichiometry of binding. Right panel shows the absorption spectra recorded during the titration. Lines are coloured from black to red to show increasing DNA concentration.

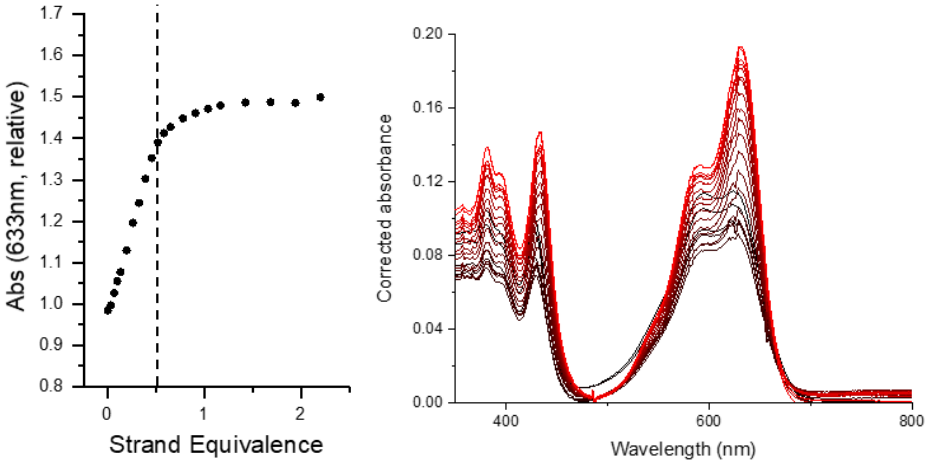

Figure S20: Absorption titration of **BDATA-M2** with c-myc DNA oligonucleotide. Left panel shows the absorbance at 633nm relative to the peak at 590-595nm for a range of DNA strand equivalences, with the vertical dashed line indicating the stoichiometry of binding. Right panel shows the absorption spectra recorded during the titration. Lines are coloured from black to red to show increasing DNA concentration.

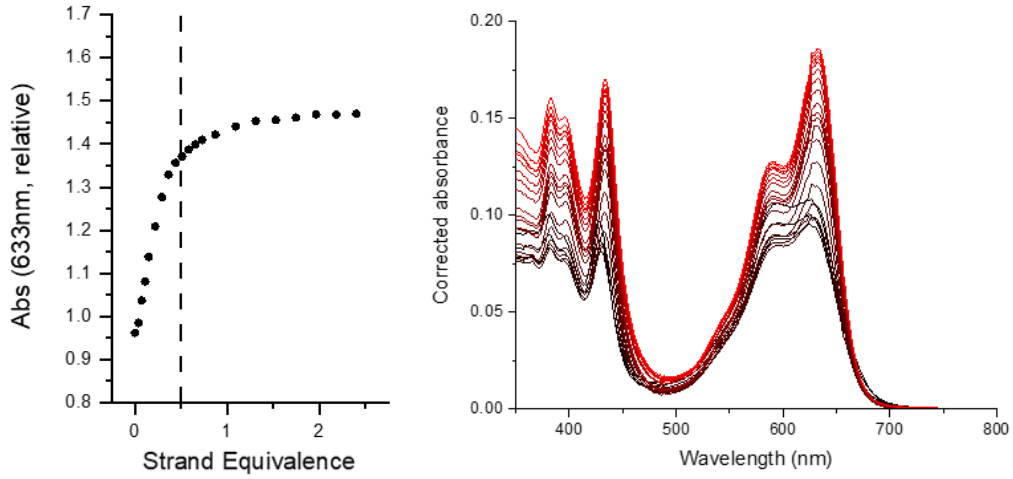

Figure S21: Absorption titration of **BDATA-M2** with HRAS-1 DNA oligonucleotide. Left panel shows the absorbance at 633nm relative to the peak at 590-595nm for a range of DNA strand equivalences, with the vertical dashed line indicating the stoichiometry of binding. Right panel shows the absorption spectra recorded during the titration. Lines are coloured from black to red to show increasing DNA concentration.

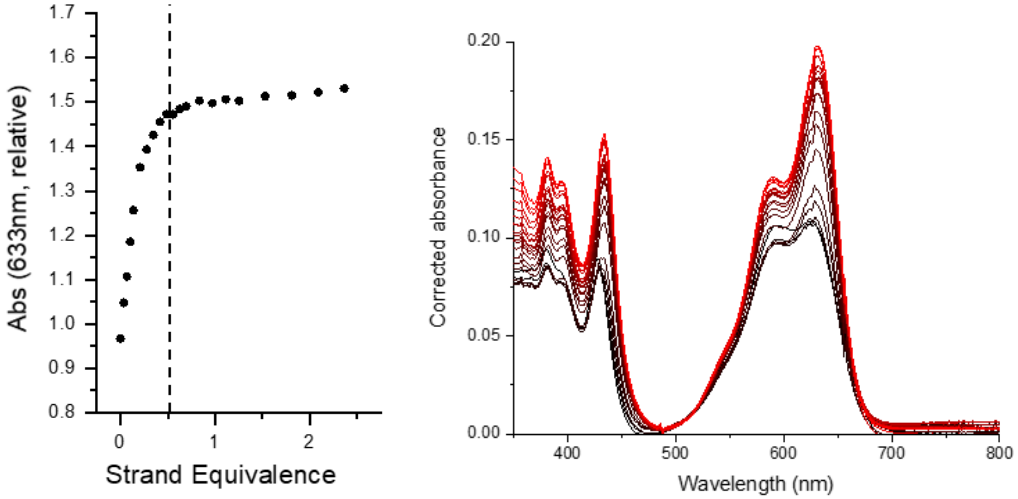

Figure S22: Absorption titration of **BDATA-M2** with HT-G4 DNA oligonucleotide. Left panel shows the absorbance at 633nm relative to the peak at 590-595nm for a range of DNA strand equivalences, with the vertical dashed line indicating the stoichiometry of binding. Right panel shows the absorption spectra recorded during the titration. Lines are coloured from black to red to show increasing DNA concentration.

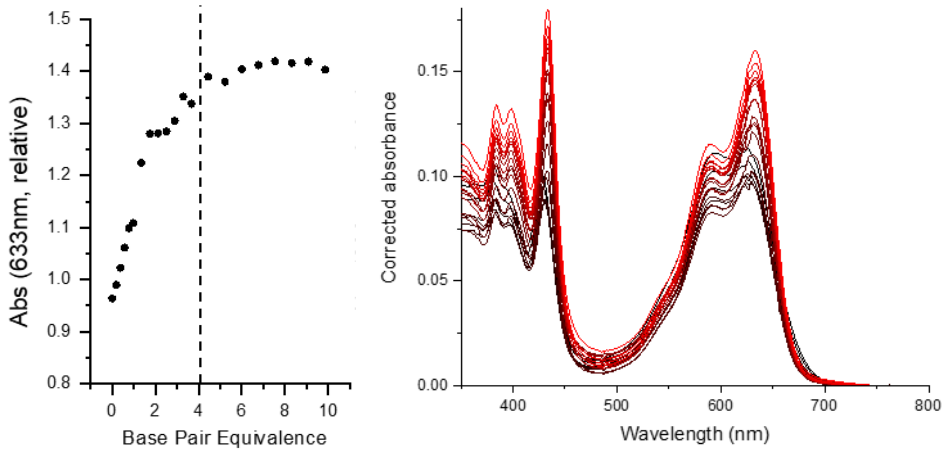

Figure S23: Absorption titration of **BDATA-M2** with CT-DNA. Left panel shows the absorbance at 633nm relative to the peak at 590-595nm for a range of DNA strand equivalences, with the vertical dashed line indicating the stoichiometry of binding. Right panel shows the absorption spectra recorded during the titration. Lines are coloured from black to red to show increasing DNA concentration.

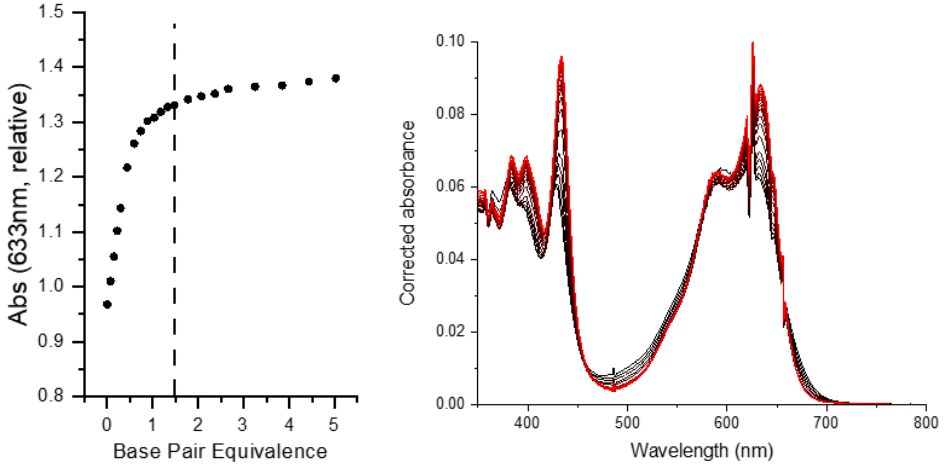

Figure S24: Absorption titration of **BDATA-M2** with ds17 dsDNA oligonucleotide. Left panel shows the absorbance at 633nm relative to 590-595nm for a range of DNA strand equivalences, with the vertical dashed line indicating the stoichiometry of binding. Right panel shows the absorption spectra recorded during the titration. Lines are coloured from black to red to show increasing DNA concentration.

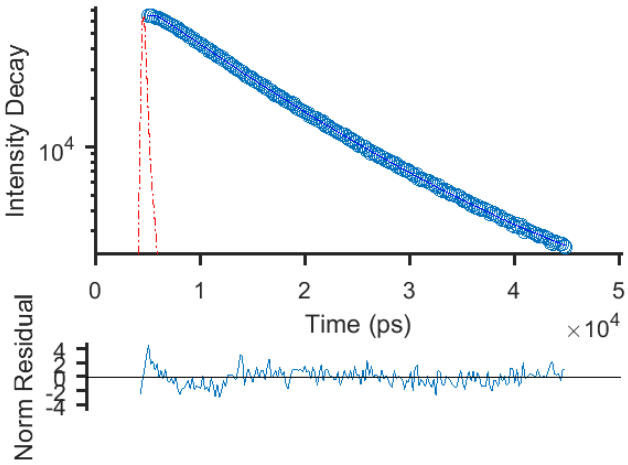

Figure S25: Time-resolved fluorescence decays recorded for **CDATA-M2** incubated with G4-forming oligonucleotide c-myc. Blue dots indicate the collected data, the blue line the fitted decay and the red dashed line the IRF prompt. Excitation at 478 nm, emission at 640 nm.

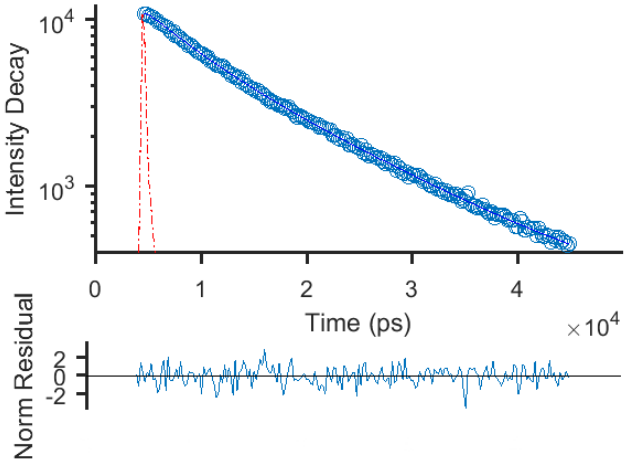

Figure S26: Time-resolved fluorescence decays recorded for **CDATA-M2** incubated with G4-forming oligonucleotide c-kit87up. Blue dots indicate the collected data, the blue line the fitted decay and the red dashed line the IRF prompt. Excitation at 478 nm, emission at 640 nm.

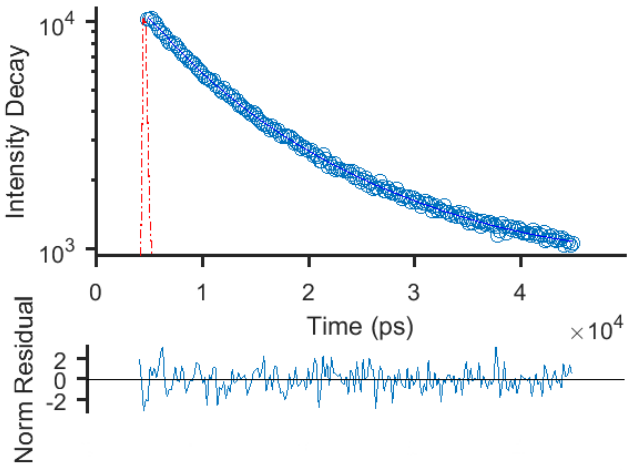

Figure S27: Time-resolved fluorescence decays recorded for **CDATA-M2** incubated with G4-forming oligonucleotide 22AG. Blue dots indicate the collected data, the blue line the fitted decay and the red dashed line the IRF prompt. Excitation at 478 nm, emission at 640 nm.

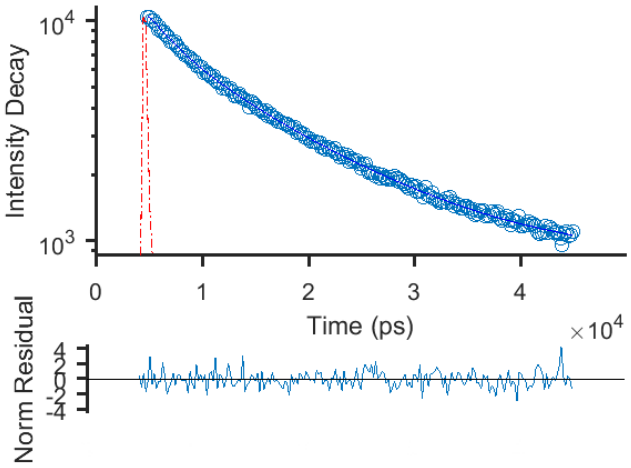

Figure S28: Time-resolved fluorescence decays recorded for **CDATA-M2** incubated with G4-forming oligonucleotide HRAS1. Blue dots indicate the collected data, the blue line the fitted decay and the red dashed line the IRF prompt. Excitation at 478 nm, emission at 640 nm.

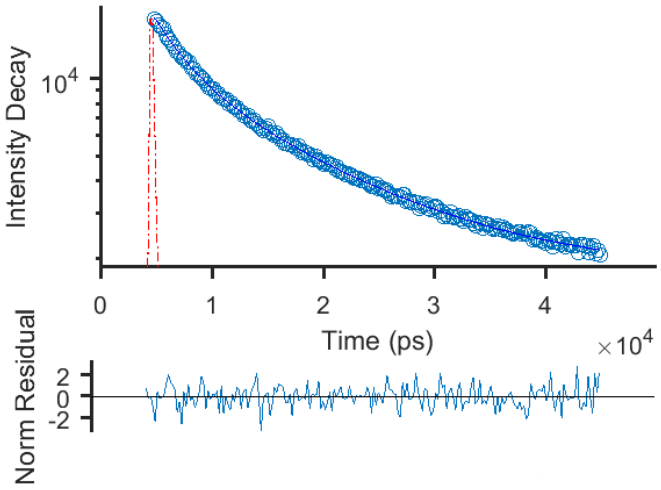

Figure S29: Time-resolved fluorescence decays recorded for **CDATA-M2** incubated with G4-forming oligonucleotide HTG4. Blue dots indicate the collected data, the blue line the fitted decay and the red dashed line the IRF prompt. Excitation at 478 nm, emission at 640 nm.

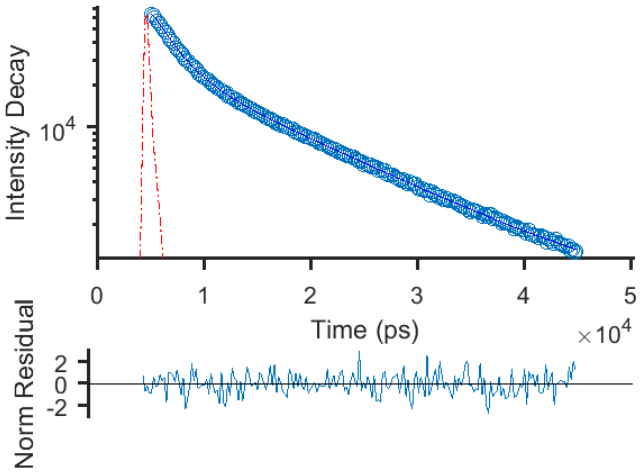

Figure S30: Time-resolved fluorescence decays recorded for **CDATA-M2** incubated with non-G4 DNA, CT-DNA. Blue dots indicate the collected data, the blue line the fitted decay and the red dashed line the IRF prompt. Excitation at 478 nm, emission at 640 nm.

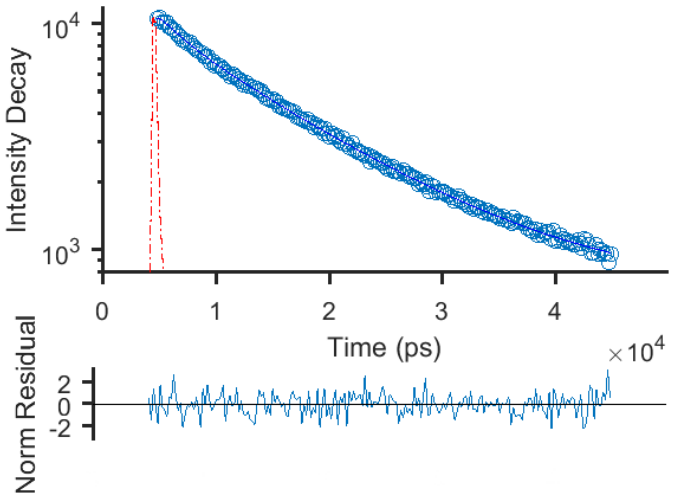

Figure S31: Time-resolved fluorescence decays recorded for **CDATA-M2** incubated with non-G4 DNA, ds17 strand 1. Blue dots indicate the collected data, the blue line the fitted decay and the red dashed line the IRF prompt. Excitation at 478 nm, emission at 640 nm.

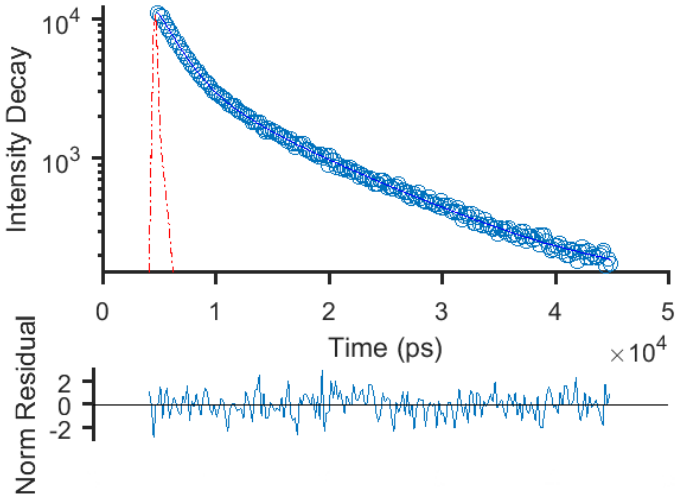

Figure S32: Time-resolved fluorescence decays recorded for **CDATA-M2** incubated with non-G4 DNA, d(AT)8. Blue dots indicate the collected data, the blue line the fitted decay and the red dashed line the IRF prompt. Excitation at 478 nm, emission at 640 nm.

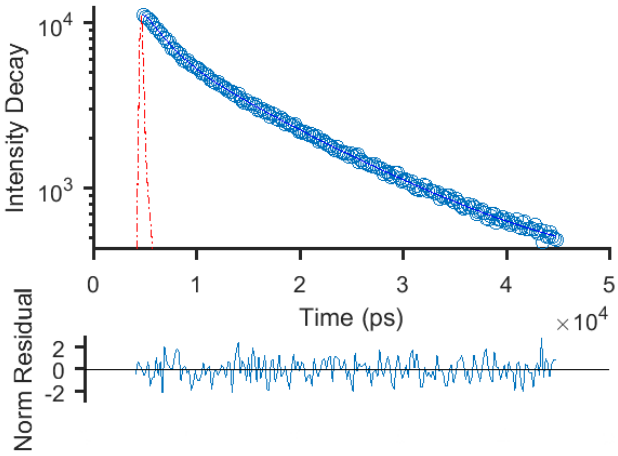

Figure S33: Time-resolved fluorescence decays recorded for **CDATA-M2** incubated with non-G4 DNA, ds17. Blue dots indicate the collected data, the blue line the fitted decay and the red dashed line the IRF prompt. Excitation at 478 nm, emission at 640 nm.

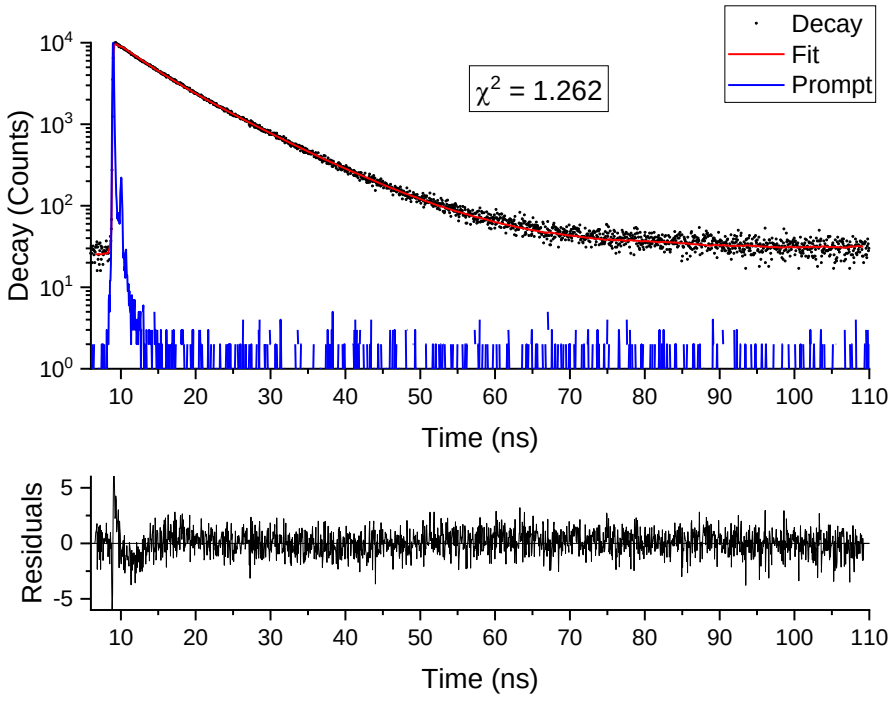

Figure S34: Time-resolved fluorescence decays recorded for **BDATA-M2** incubated with G4-forming oligonucleotide c-myc. Black dots indicate the collected data, the red line the fitted decay and the blue line the IRF prompt. Excitation at 404 nm, emission at 660 nm.

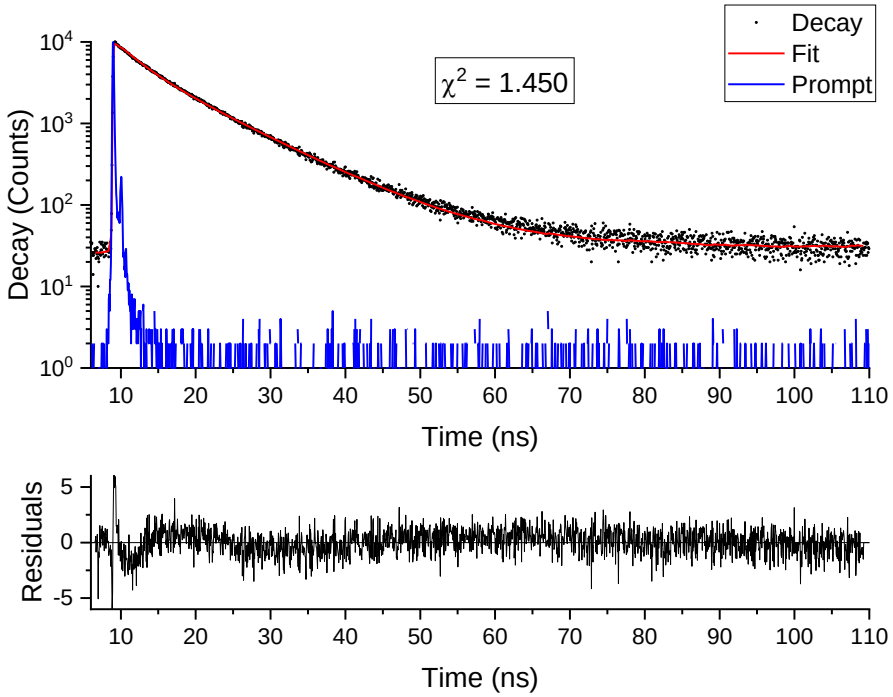

Figure S35: Time-resolved fluorescence decays recorded for **BDATA-M2** incubated with G4-forming oligonucleotide c-kit87up. Black dots indicate the collected data, the red line the fitted decay and the blue line the IRF prompt. Excitation at 404 nm, emission at 660 nm.

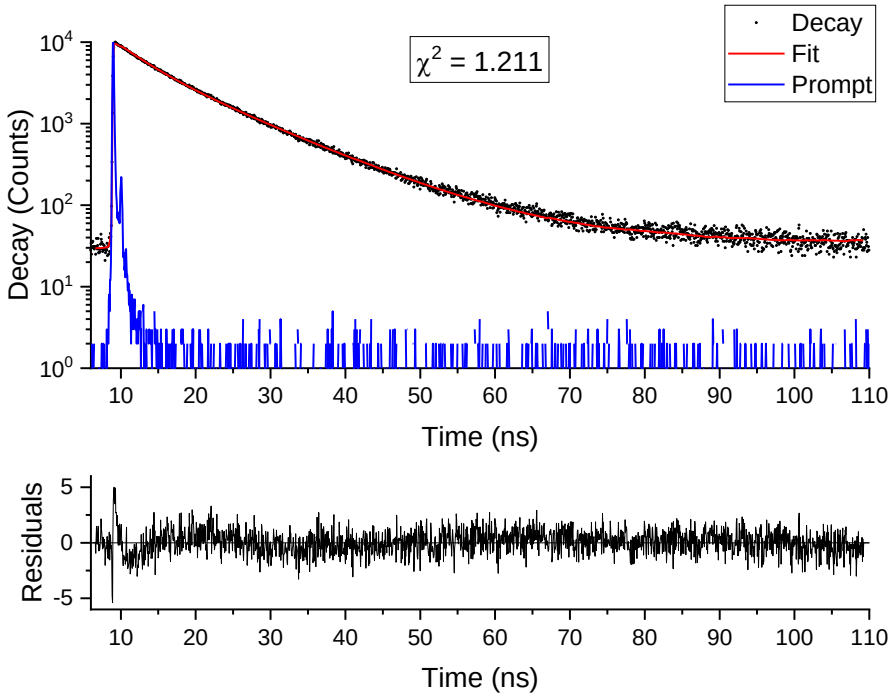

Figure S36: Time-resolved fluorescence decays recorded for **BDATA-M2** incubated with G4-forming oligonucleotide 22AG. Black dots indicate the collected data, the red line the fitted decay and the blue line the IRF prompt. Excitation at 404 nm, emission at 660 nm.

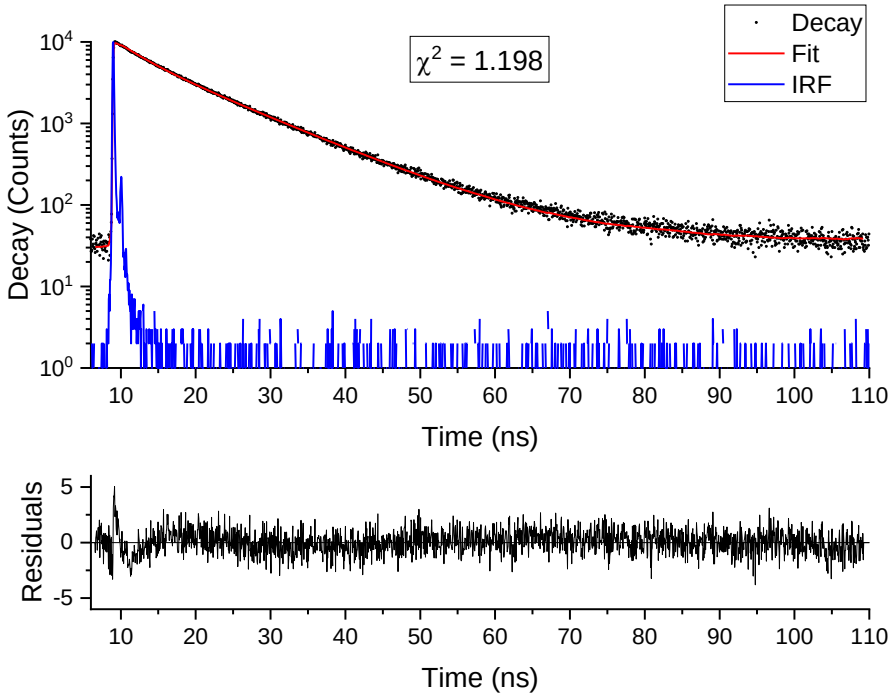

Figure S37: Time-resolved fluorescence decays recorded for **BDATA-M2** incubated with G4-forming oligonucleotide HRAS-1. Black dots indicate the collected data, the red line the fitted decay and the blue line the IRF prompt. Excitation at 404 nm, emission at 660 nm.

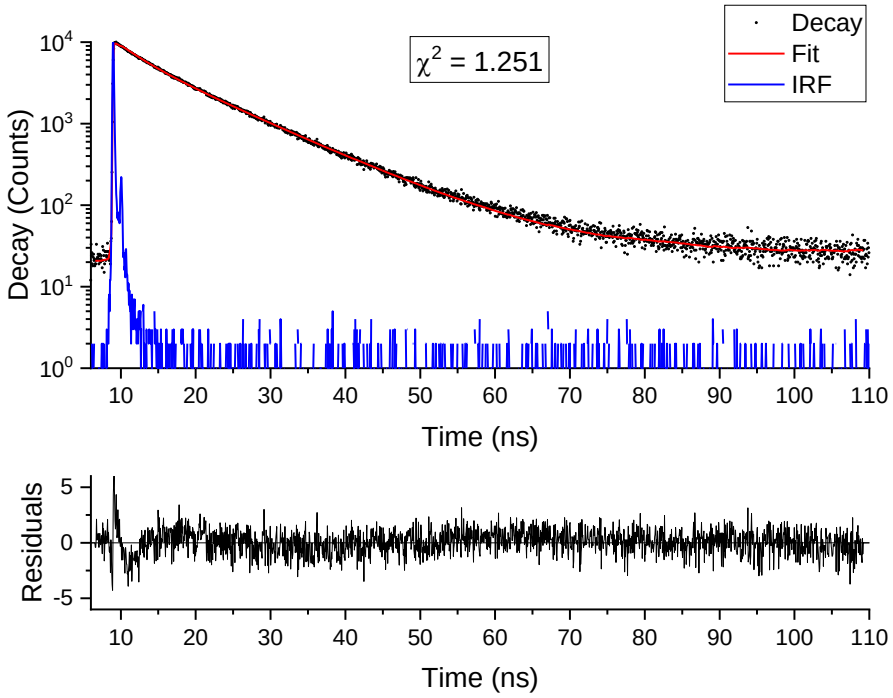

Figure S38: Time-resolved fluorescence decays recorded for **BDATA-M2** incubated with G4-forming oligonucleotide HT-G4. Black dots indicate the collected data, the red line the fitted decay and the blue line the IRF prompt. Excitation at 404 nm, emission at 660 nm.

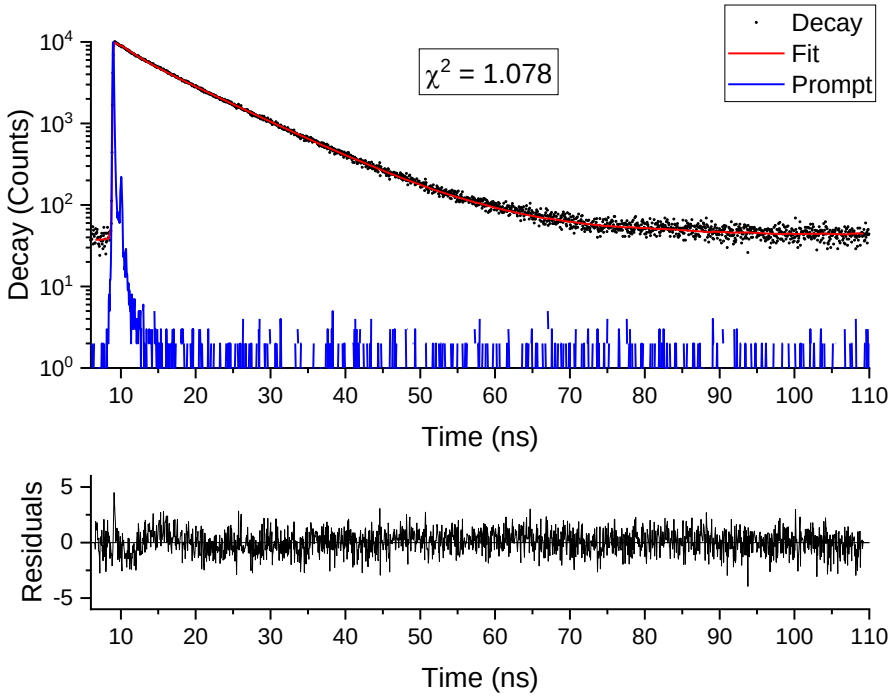

Figure S39: Time-resolved fluorescence decays recorded for **BDATA-M2** incubated with non G4-forming DNA, CT-DNA. Black dots indicate the collected data, the red line the fitted decay and the blue line the IRF prompt. Excitation at 404 nm, emission at 660 nm.

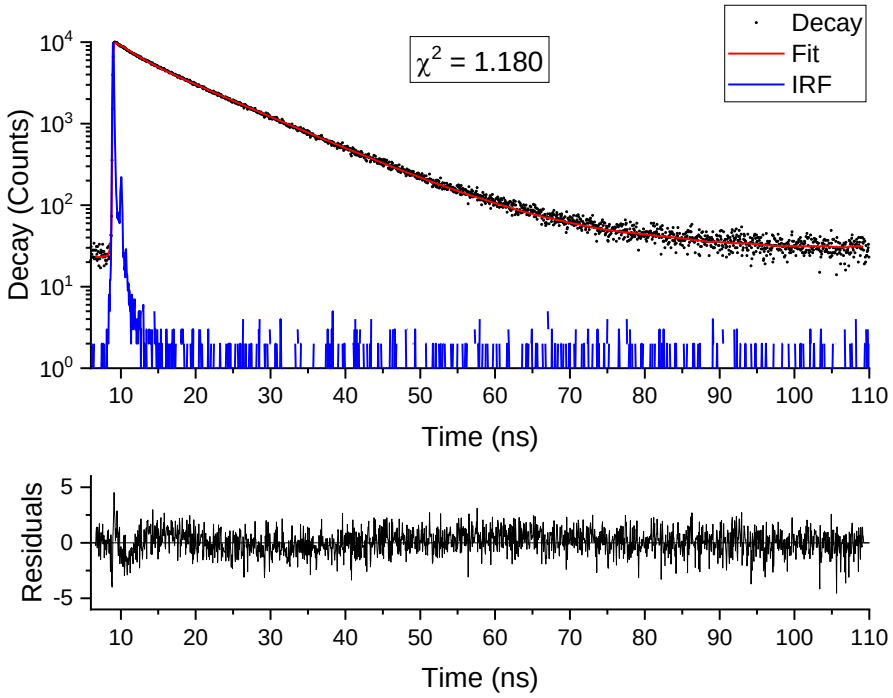

Figure S40: Time-resolved fluorescence decays recorded for **BDATA-M2** incubated with non G4-forming DNA, ds17 strand 1. Black dots indicate the collected data, the red line the fitted decay and the blue line the IRF prompt. Excitation at 404 nm, emission at 660 nm.

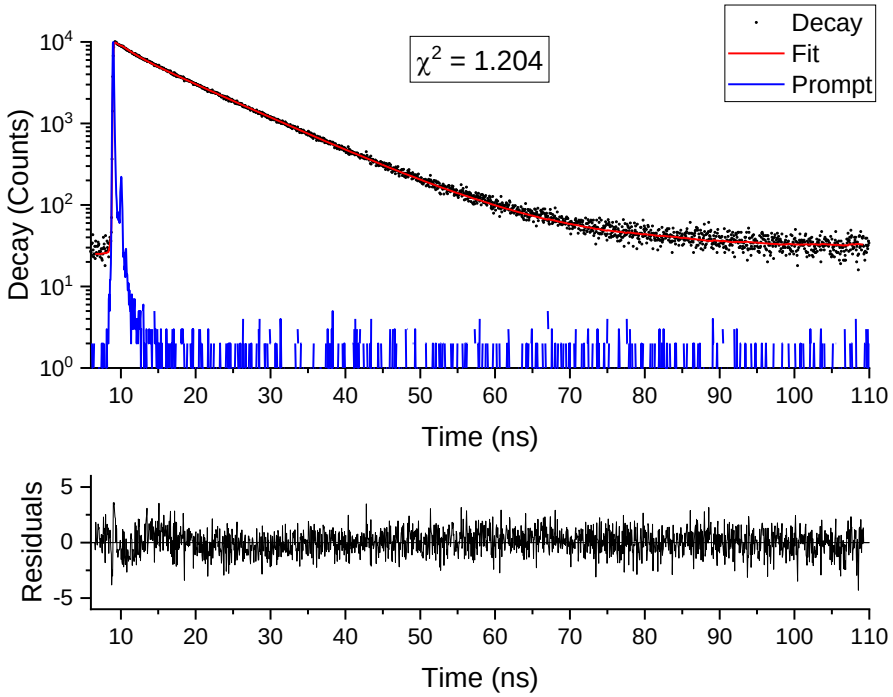

Figure S41: Time-resolved fluorescence decays recorded for **BDATA-M2** incubated with non G4-forming DNA, d(AT)8. Black dots indicate the collected data, the red line the fitted decay and the blue line the IRF prompt. Excitation at 404 nm, emission at 660 nm.

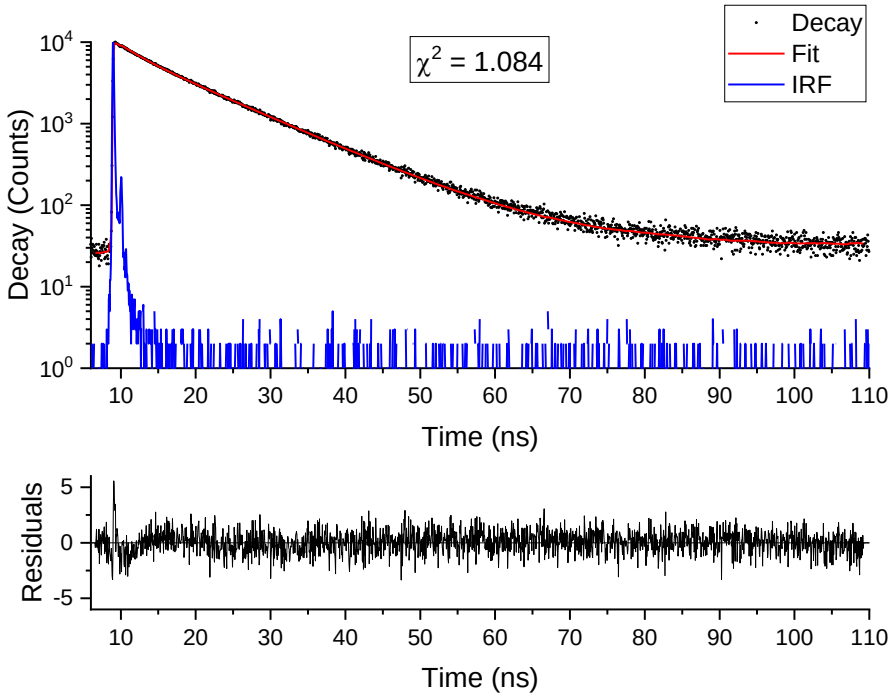

Figure S42: Time-resolved fluorescence decays recorded for **BDATA-M2** incubated with non G4-forming DNA, ds17. Black dots indicate the collected data, the red line the fitted decay and the blue line the IRF prompt. Excitation at 404 nm, emission at 660 nm.

Table S1: Binding affinities of **CDATA-M2** and **BDATA-M2** as determined by fluorescence emission titrations.

Oligonucleotide	**CDATA-M2 K_a ($x10^5$ M^{-1})**	**BDATA-M2 K_a ($x10^5$ M^{-1})**
c-myc	36 ± 17	38 ± 7.8
c-kit87up	6.6 ± 2.2	0.93 ± 0.17
HRAS-1	0.41 ± 0.18	14 ± 4.5
CT-DNA	0.40 ± 0.20	44 ± 5.2
ds17	1.3 ± 0.085	73 ± 14

Table S2: FLT fitting data for **CDATA-M2** bound to oligonucleotide DNA.

Oligonucleotide	**t1 (ns)**	**a1 (%)**	**t2 (ns)**	**a2 (%)**	**tw (ns)**	**chi2**
c-myc	8.7	86	20.2	14	11.8	1.48
c-kit87up	4.7	44	13.1	56	11.2	1.03
22AG	4.2	47	12.2	53	10.3	1.26
HRAS-1	2.6	35	12.0	65	11.0	1.19
HT-G4	2.8	53	12.9	47	10.9	1.06
ds17 strand 1	2.1	23	12.2	77	11.7	1.04
dAT8	2.0	77	10.8	23	7.3	1.12
ds17	2.2	50	11.9	50	10.5	1.02
CT-DNA	2.1	68	11.9	32	9.3	1.03

Table S3: FLT fitting data for **BDATA-M2** bound to oligonucleotide DNA.

Oligonucleotide	**t1 (ns)**	**a1 (%)**	**t2 (ns)**	**a2 (%)**	**tw (ns)**	**chi2**
c-myc	4.3	24	9.6	76	9.0	1.26
c-kit87up	3.2	21	9.4	79	8.9	1.45
22AG	4.2	24	11.2	76	10.5	1.21
HRAS-1	3.6	13	11.2	87	10.9	1.20
HT-G4	3.5	14	10.6	86	10.2	1.25
ds17 strand 1	2.2	7	10.9	93	10.7	1.18
dAT8	1.9	5	10.5	95	10.4	1.20
ds17	2.8	7	10.7	93	10.6	1.08
CT-DNA	2.2	6	9.8	94	9.7	1.08

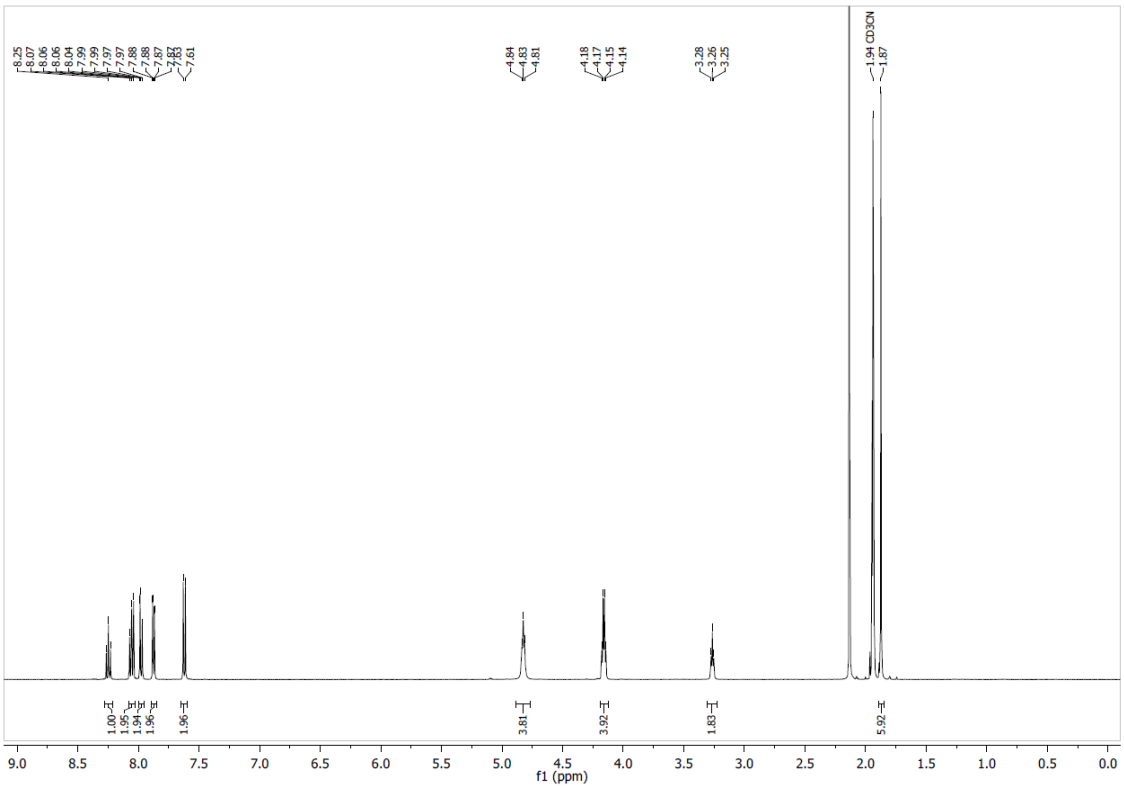

Figure S43. ^{1}H-NMR of **1** in CD_3CN at 500 MHz.

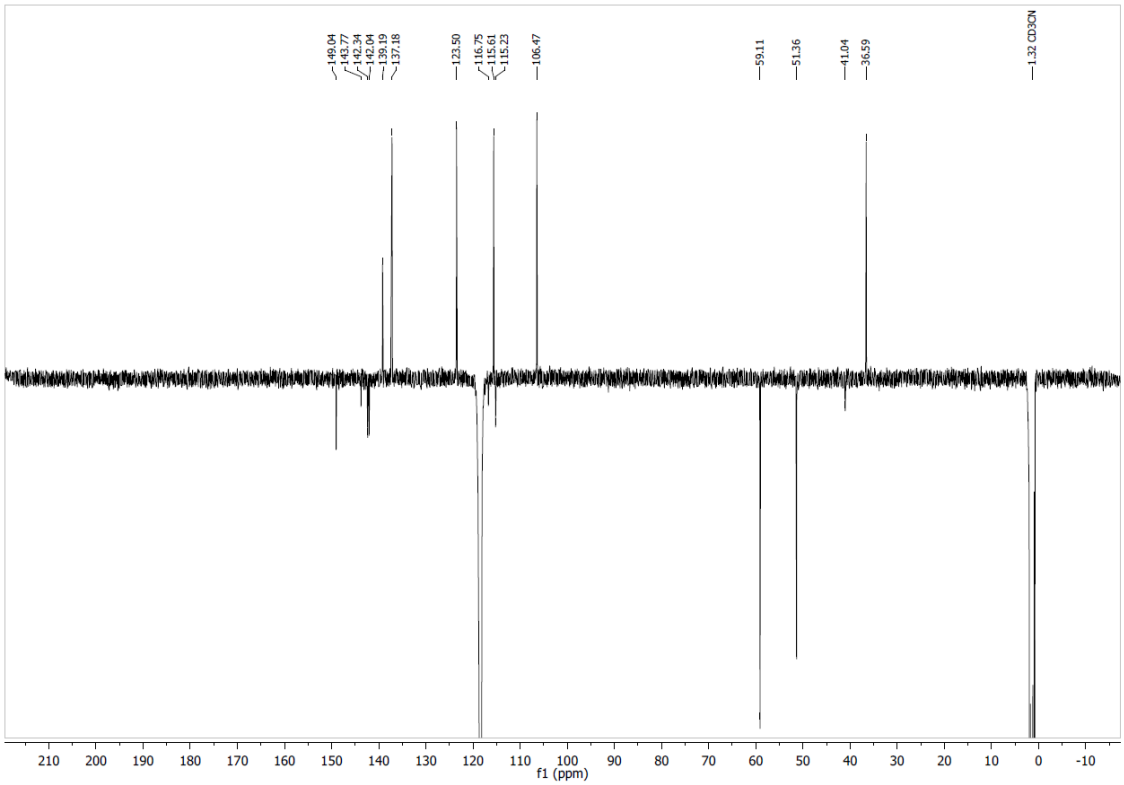

Figure S44. ^{13}C-NMR-APT of **1** in CD_3CN at 126 MHz. Spectrum is phased to show nuclei with an uneven number of protons as positive.

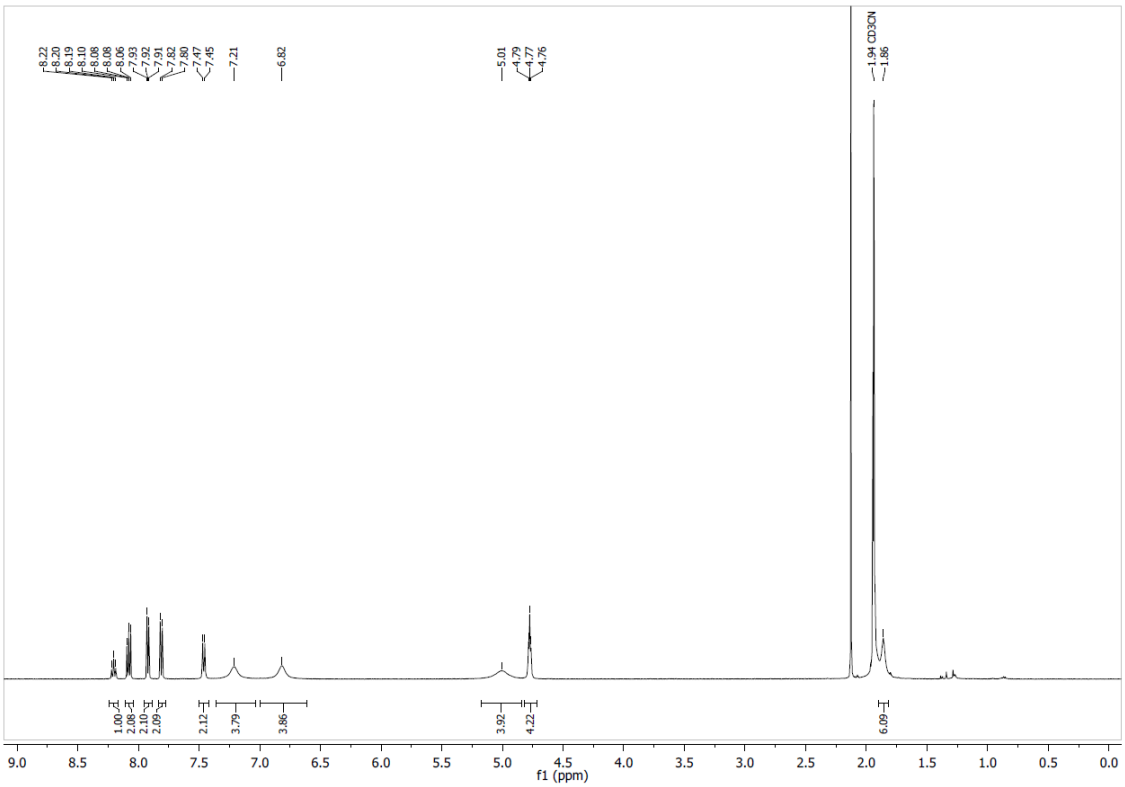

Figure S45. ^{1}H-NMR of **2** in CD_3CN at 500 MHz.

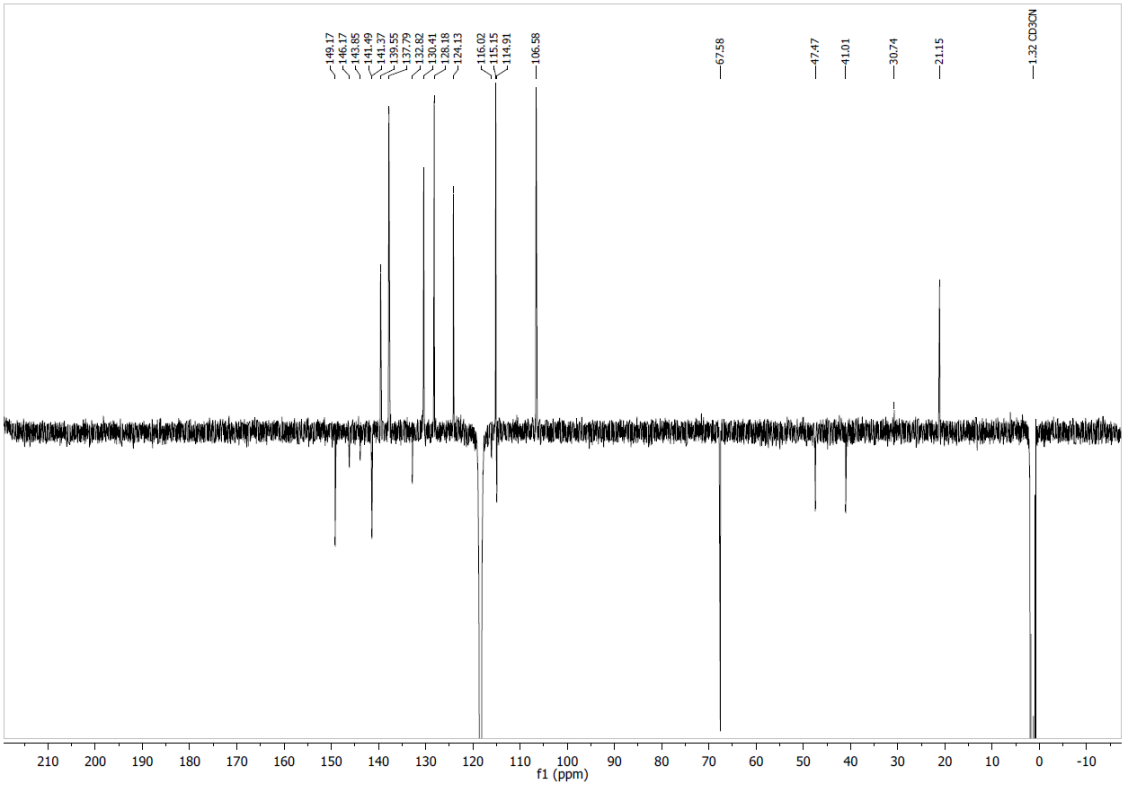

Figure S46. ^{13}C-NMR-APT of **2** in CD_3CN at 126 MHz. Spectrum is phased to show nuclei with an uneven number of protons as positive.

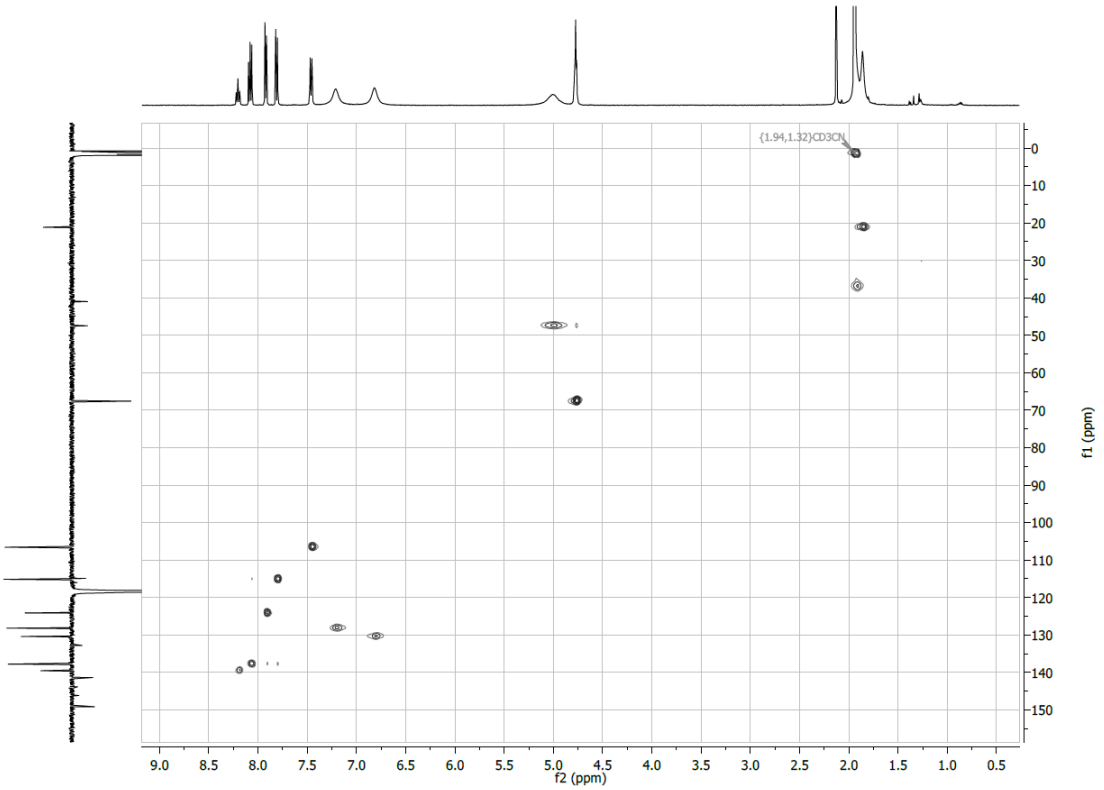

Figure S47. ^{13}C-HSQC of **2** in CD_3CN at 126 MHz in the f1 dimension and 500 MHz in the f2 dimension. This spectrum shows the cross-peak at {1.91, 36.8} corresponding to the methyl of the *para*-toluenesulfonyl group. The ^{1}H-NMR signal is obscured by the solvent and the ^{13}C-NMR peak does not resolve in the 1D-spectrum.

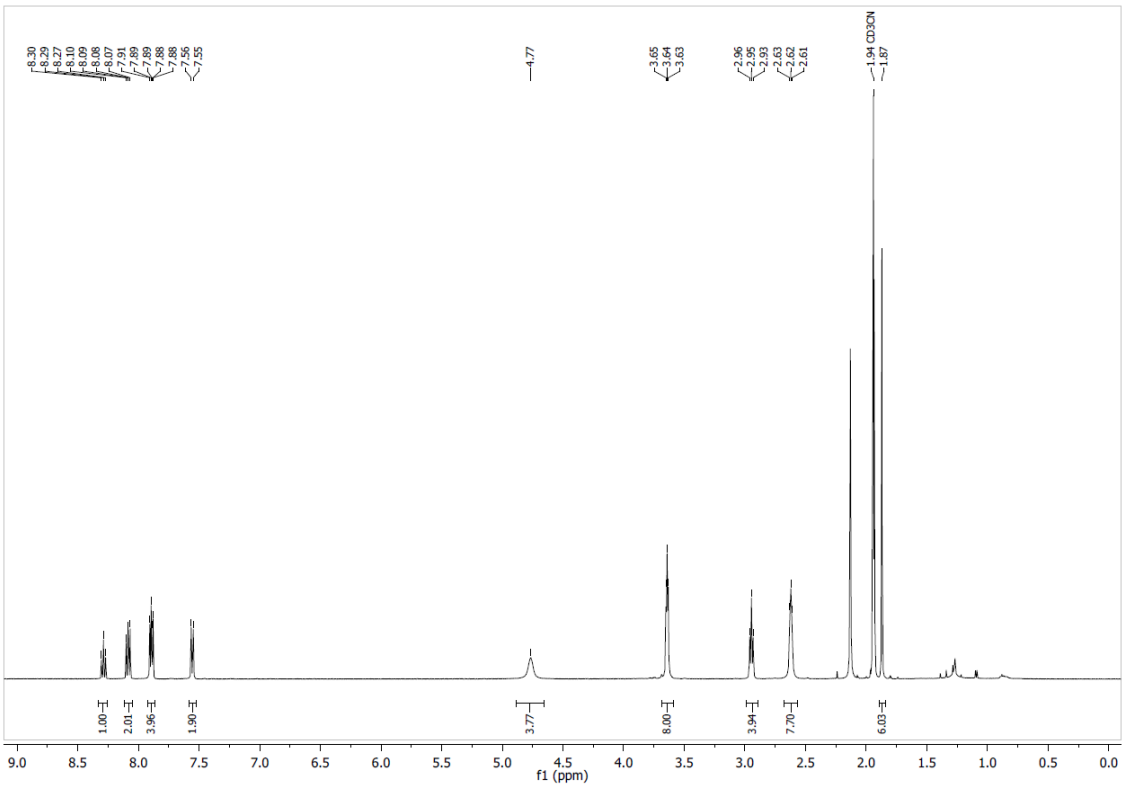

Figure S48. ^{1}H-NMR of **CDATA-M2** in CD_3CN at 500 MHz.

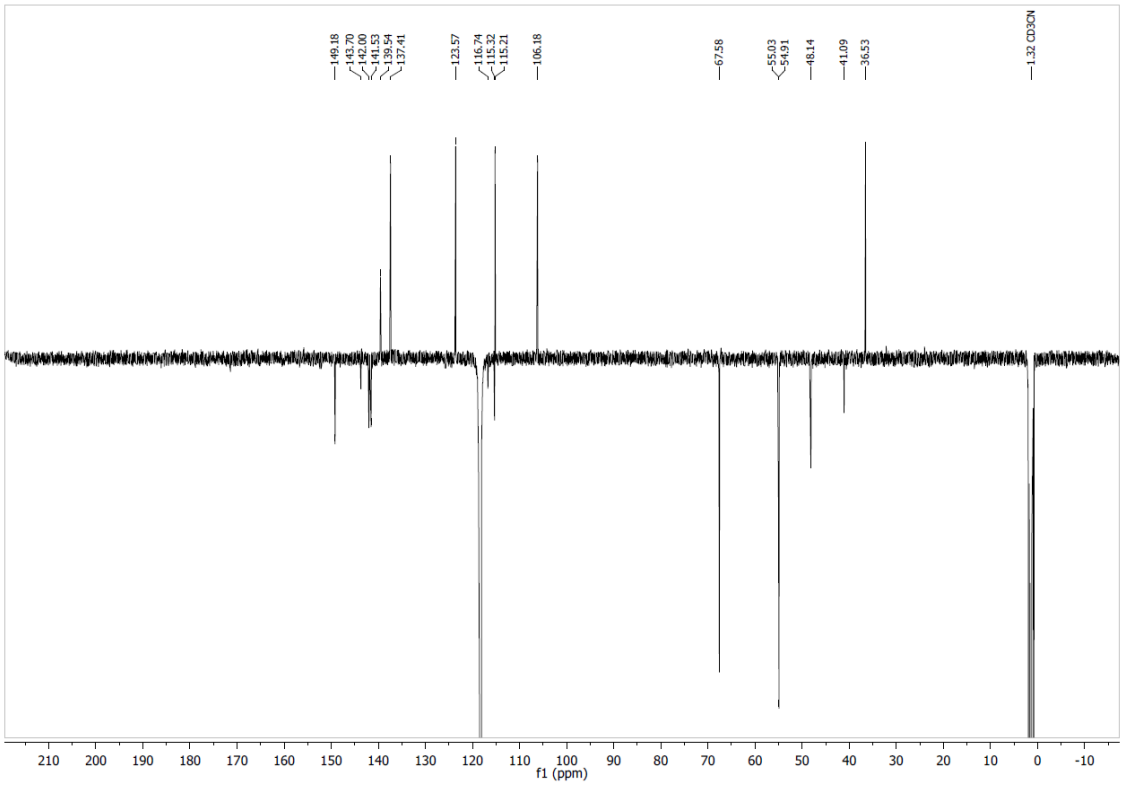

Figure S49. ^{13}C-NMR-APT of **CDATA-M2** in CD_3CN at 126 MHz. Spectrum is phased to show nuclei with an uneven number of protons as positive.

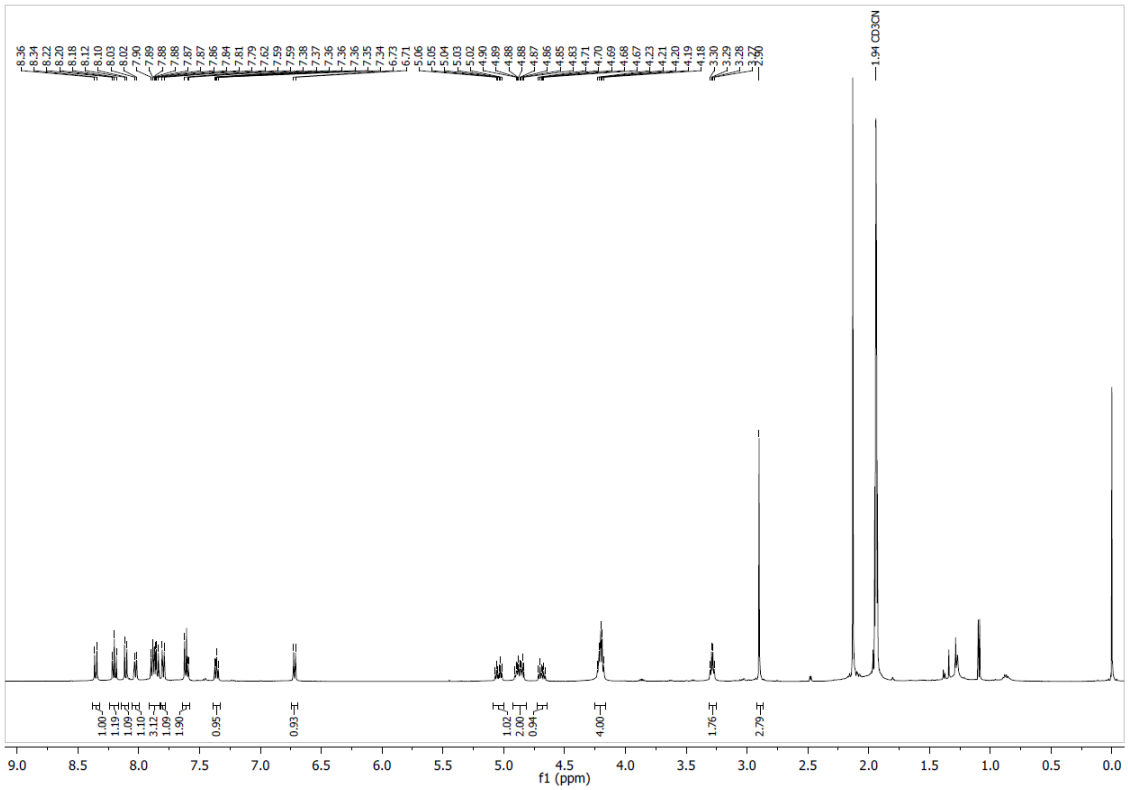

Figure S50. ^{1}H-NMR of **4** in CD_3CN at 500 MHz.

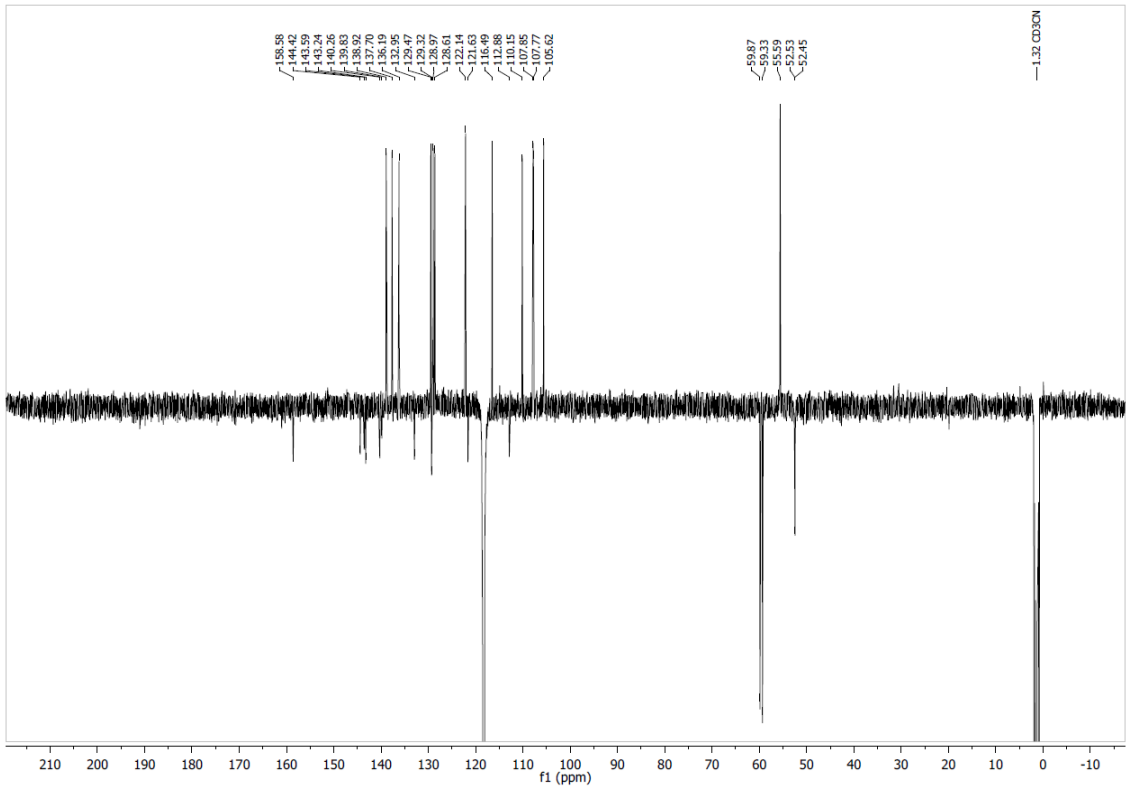

Figure S51. ^{13}C-NMR-APT of **4** in CD_3CN at 126 MHz. Spectrum is phased to show nuclei with an uneven number of protons as positive.

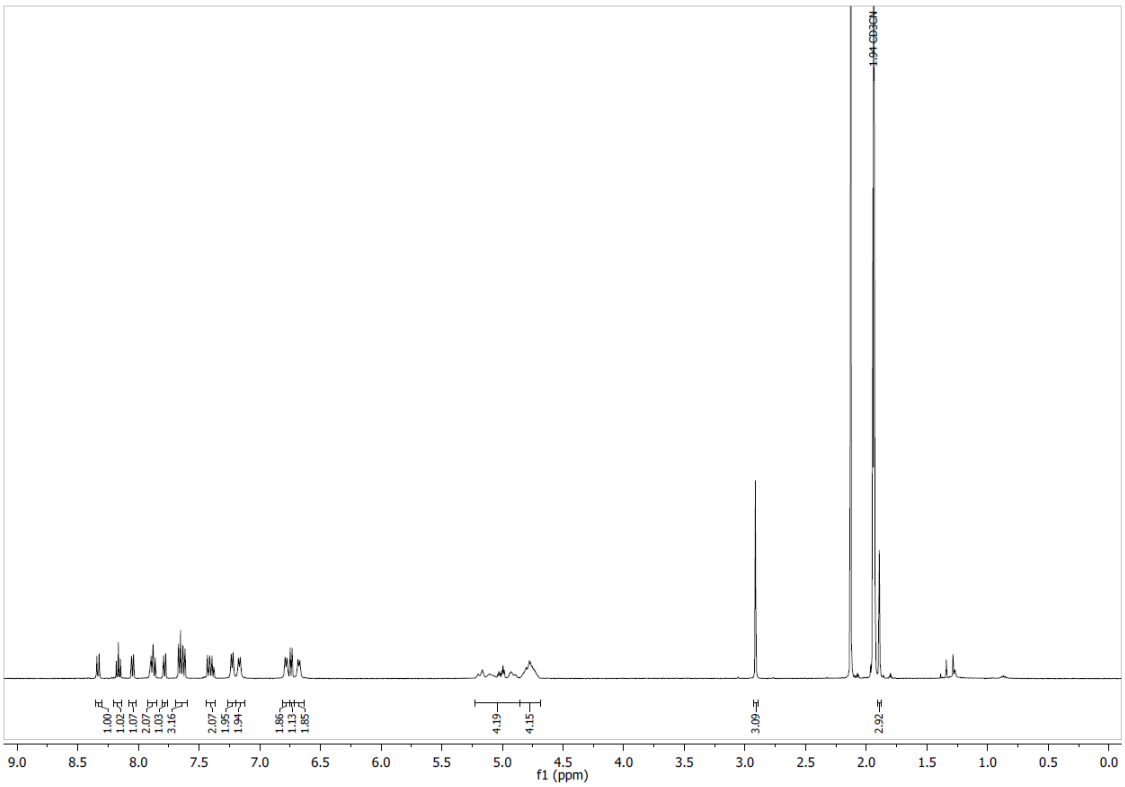

Figure S52. ^{1}H-NMR of **5** in CD_3CN at 500 MHz.

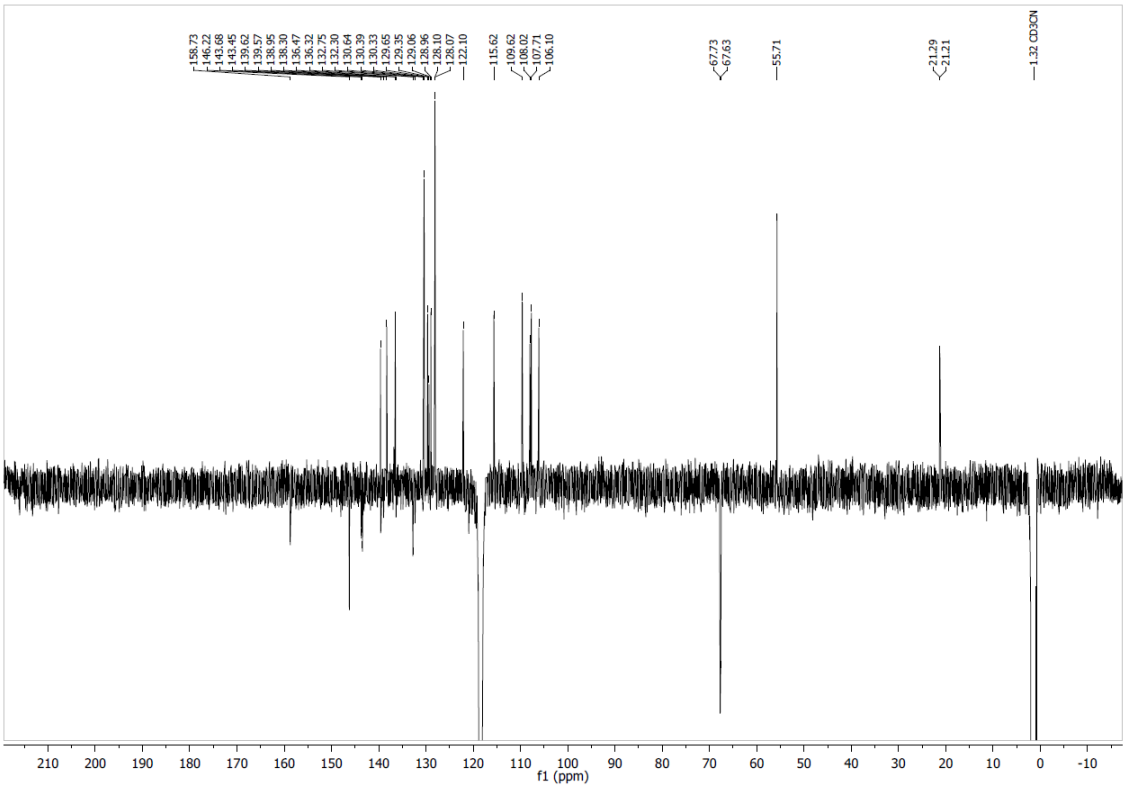

Figure S53. ^{13}C-NMR-APT of **5** in CD_3CN at 126 MHz. Spectrum is phased to show nuclei with an uneven number of protons as positive.

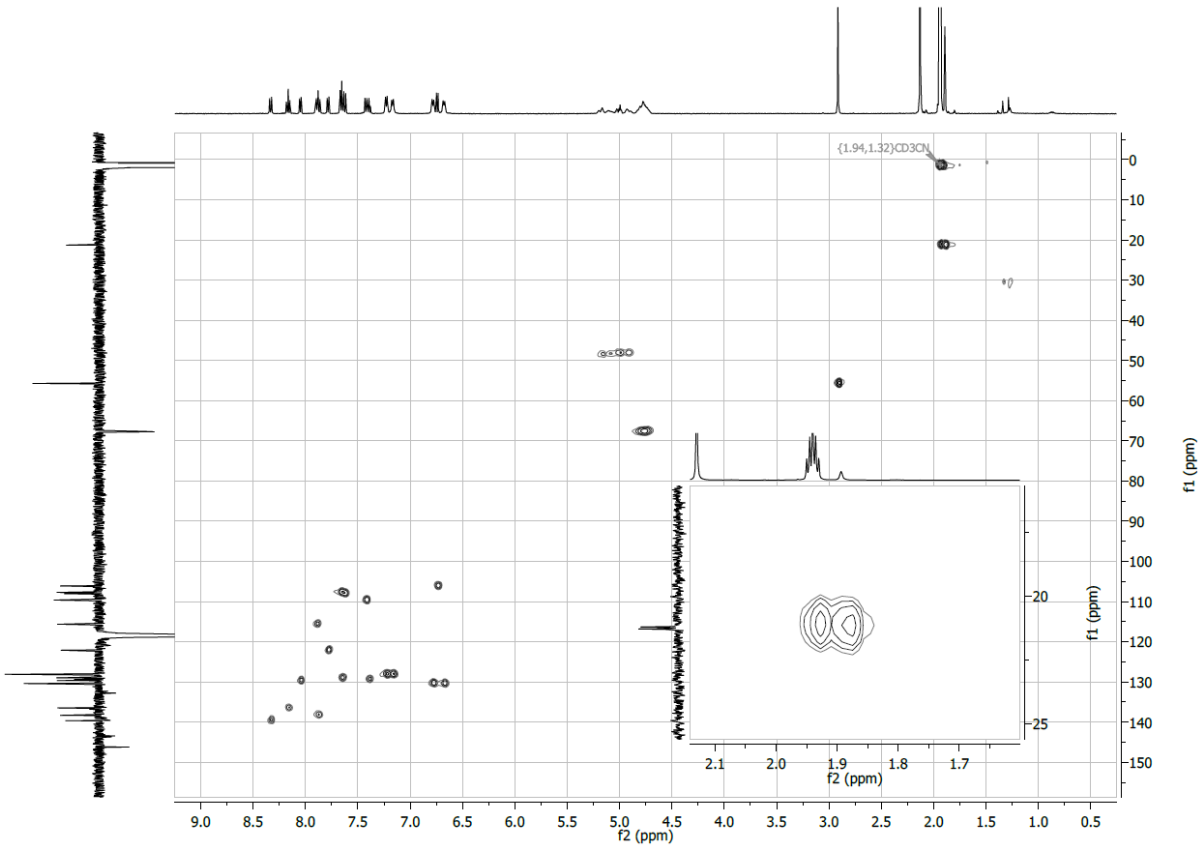

Figure S54. ^{13}C-HSQC of **5** in CD_3CN at 126 MHz in the f1 dimension and 500 MHz in the f2 dimension. The cross-peak at {1.93, 21.2} (zoom) shows how the ^{1}H-NMR signal of a methyl of the *para*-toluenesulfonyl groups is obscured by the solvent residual peak. The cross-peaks at {5.16, 48.4}, {5.09, 48.3}, {4.99, 48.1} and {4.91, 48.0} show how the α-carbons of the alkyl side chains do not give rise to ^{13}C-NMR signals in the 1D-spectrum.

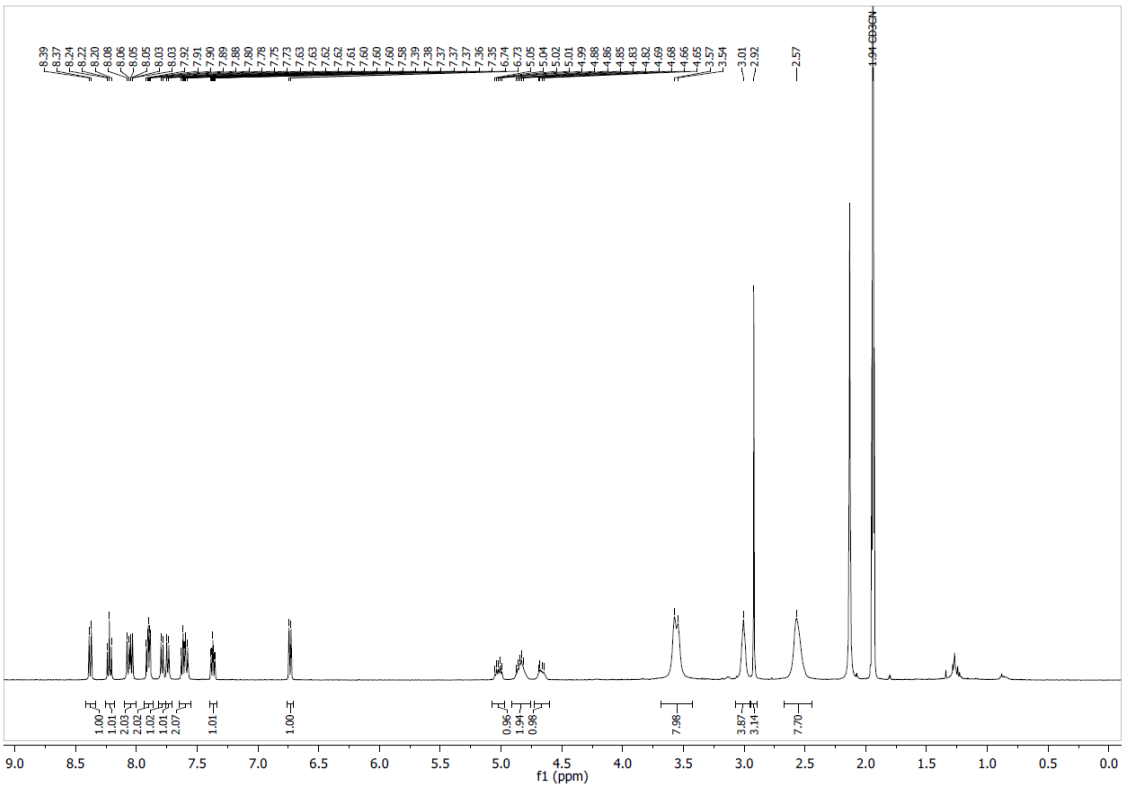

Figure S55. ^{1}H-NMR of **6** in CD_3CN at 500 MHz.

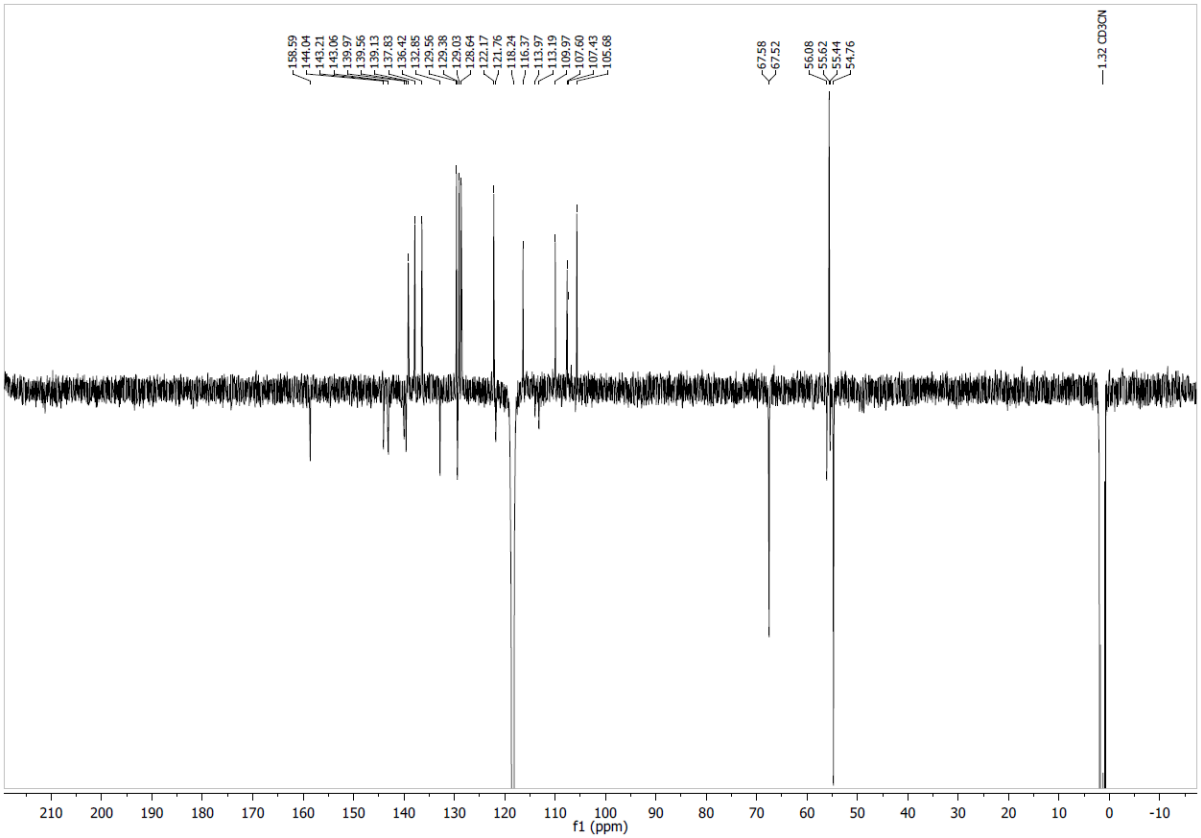

Figure S56. ^{13}C-NMR-APT of **6** in CD_3CN at 126 MHz. Spectrum is phased to show nuclei with an uneven number of protons as positive.

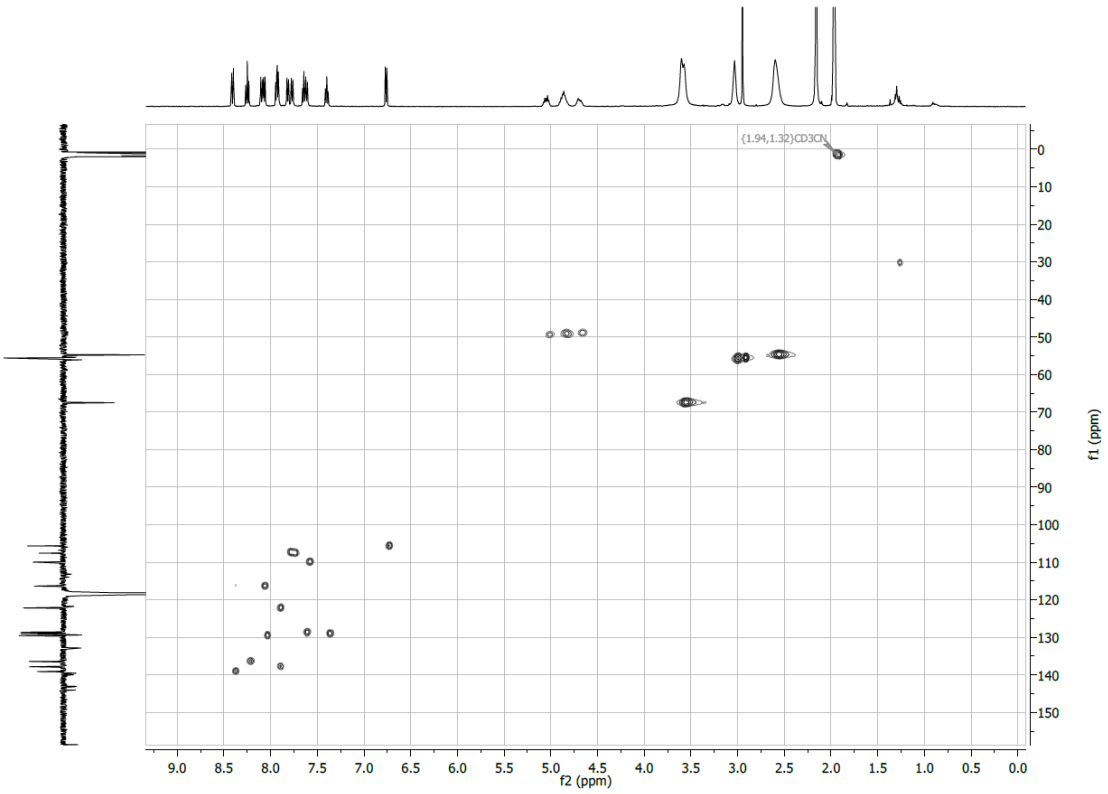

Figure S57. ^{13}C-HSQC of **6** in CD_3CN at 126 MHz in the f1 dimension and 500 MHz in the f2 dimension. The cross-peaks at {5.01, 49.4}, {4.83, 49.1} and {4.66, 49.0} show how the α-carbons of the alkyl side chains do not give rise to ^{13}C-NMR signals in the 1D-spectrum.

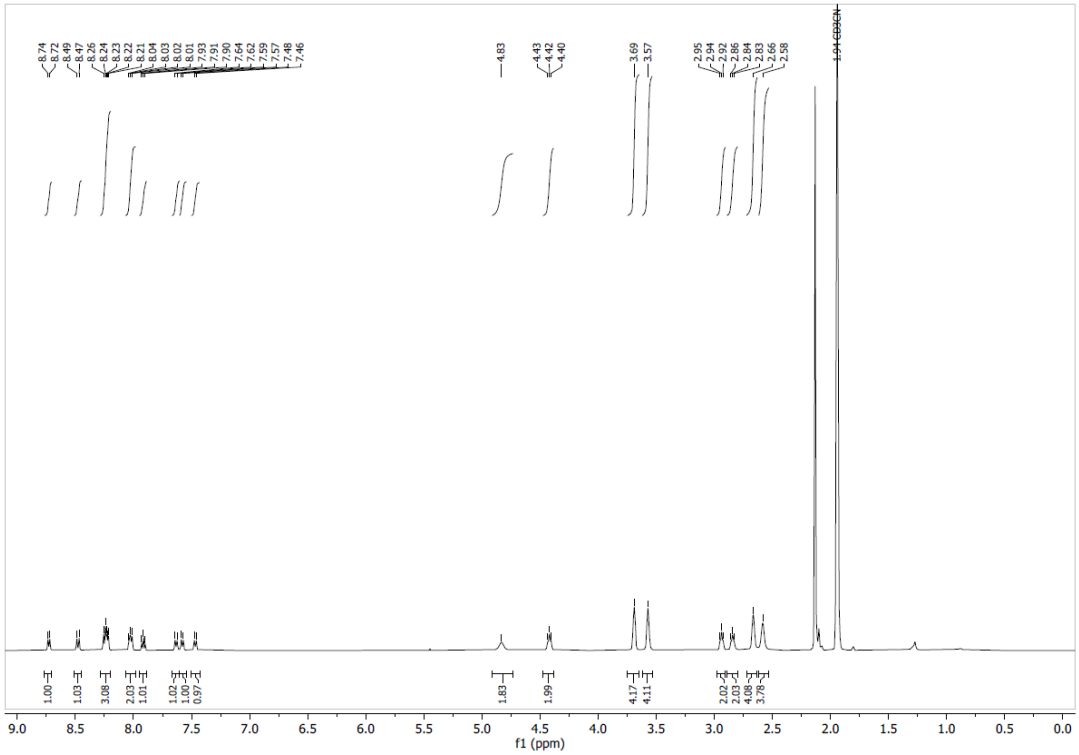

Figure S58.[1]H-NMR of **BDATA-M2** in CD_3CN at 500 MHz.

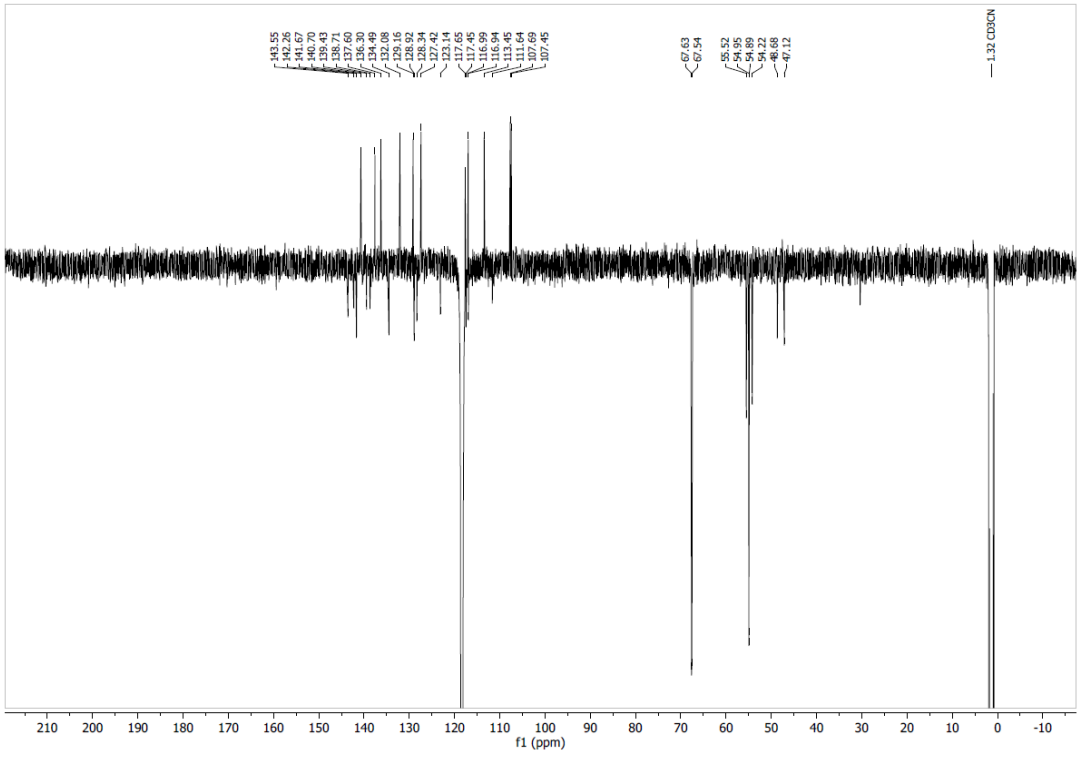

Figure S59.[13]C-NMR-APT of **BDATA-M2** in CD_3CN at 126 MHz. Spectrum is phased to show nuclei with an uneven number of protons as positive.

General details for cell culture: U2OS bone osteosarcoma cells were cultured in Dulbecco's Modified Eagle Media containing 10% foetal bovine serum. Cells were incubated at 37 ^{o}C in an atmosphere of 5% carbon dioxide.

Experimental details for cell viability: MTS Reagent Powder (Promega) was dissolved in sterile PBS as a 2 mg/mL solution. Phenazine methosulfate (PMS, Sigma Life Science) was dissolved in PBS as a 0.92 mg/mL solution. On the day of experiment, 3 mL of MTS solution was mixed with 150 µL of PMS and 3 mL of the resulting solution was mixed with 15 mL of media. U2OS cells were added to a 96-well plate, with 5000 cells per well in 100 µL of medium. After 24 h, cells were washed with PBS and fresh medium was added containing 0.1-100 µM of triangulenium dye. After a further 24h, the medium was replaced with medium containing MTS/PMS (100 µL). The cells were incubated for 2 h and absorbance at 490 nm was measured (BMG LABTECH, CLARIOstar Plus). Absorbance at 630 nm was subtracted to correct for background. Results reported are the average of three technical replicates for each concentration. Viability was calibrated using a DMSO-only control as 100% and wells containing no cells as 0%.

Experimental details for cell localisation imaging: For confocal imaging, 30000 cells were added to chambered culture slide in 250 µL of media containing triangulenium dye. Concentration and incubation time were 10 µM and 24 h unless otherwise stated. For co-staining experiments, 10 mg/mL Hoechst 33342 in water was added at a 1:2000 dilution to stain cell nuclei, LysoTracker Green DND-26 was added at final concentration 50 nM to stain cell lysosomes and MitoTracker Orange CMTMRos was added at final concentration 50 nM to

stain cell mitochondria. Co-stains were incubated for at least 30 minutes before imaging. Cells were imaged by confocal microscopy using an inverted confocal laser scanning microscope (Leica, SP5 II). Samples on the microscope stage were heated by a thermostat (Lauda GmbH, E200) to 37°C, and kept under an atmosphere of 5% CO_2 in air. A 100x (oil, NA = 1.4) objective was used to collect images at 512x512 resolution. Generally, unless otherwise stated, for imaging **BDATA-M2**, a 633 nm internal laser was used, and fluorescence was detected from 650-700 nm, and for imaging **CDATA-M2**, a 514 nm internal laser was used, and fluorescence was detected at 550-700 nm.

For co-staining experiments, **CDATA-M2** was instead excited using a 633 nm internal laser to avoid bleedthrough. For imaging Hoechst 33342 a Coherent Chameleon Vision II laser was used at 760 nm to achieve a two-photon excitation of the fluorophore, with fluorescence detected at 400-500 nm, with trianguleniums detected at 650-690 nm. For imaging LysoTracker Green, a 476 nm internal laser was used for excitation, with detection at 500-530 nm, with trianguleniums detected at 640-750 nm for **CDATA-M2** and 660-750 nm for **BDATA-M2**. For imaging MitoTracker Orange, a 514 nm internal laser was used for excitation, with detection at 535-575 nm, with trianguleniums detected at 640-750 nm for **CDATA-M2** and 660-750 nm for **BDATA-M2**. In the case of MitoTracker Orange, the two channels were acquired separately to prevent appearance of MitoTracker signal in the triangulenium channel.

Experimental details for fluorescence lifetime imaging microscopy (FLIM): FLIM on U2OS cells stained with **BDATA-M2** (10 μM, 24 h) was performed by time-correlated single-photon counting (TCSPC) with an SPC-830 single-photon counting card (Becker & Hickl GmbH) and an

inverted confocal laser scanning microscope (Leica, SP5 II). Cells were incubated at 37 °C with 5% CO2 in air whilst on the microscope stage, heated by a thermostat (Lauda GmbH, E200). excited with a pulsed diode laser (Becker & Hickl GmbH, 633 nm, 20 MHz) with a PMC-100-1 photomultiplier tube (Hamamatsu) detector. Emitted photons (650-700 nm) were collected for 1000s using a 100x (oil, NA = 1.4) objective at 256 x 256 resolution. An IRF was recorded using reflection of the excitation beam from a glass cover slide. Lifetime data were fitted using FLIMfit (v5.1.1, Sean Warren, Imperial College London). Data was binned using 7 x 7 square binning and decays were fit using a bi-exponential function with a scatter parameter added to account for scattered excitation photons. A mask was applied to the image to only analyse the nucleus of each cell. To ensure reliable fitting, only nuclei with a minimum of 300 counts at the peak of the decay were used in analysis and fitting data was considered reliable where the goodness-of-fit as measured by $\chi 2$ was below 2. Intensity-weighted average lifetime was determined as in TCSPC experiments.

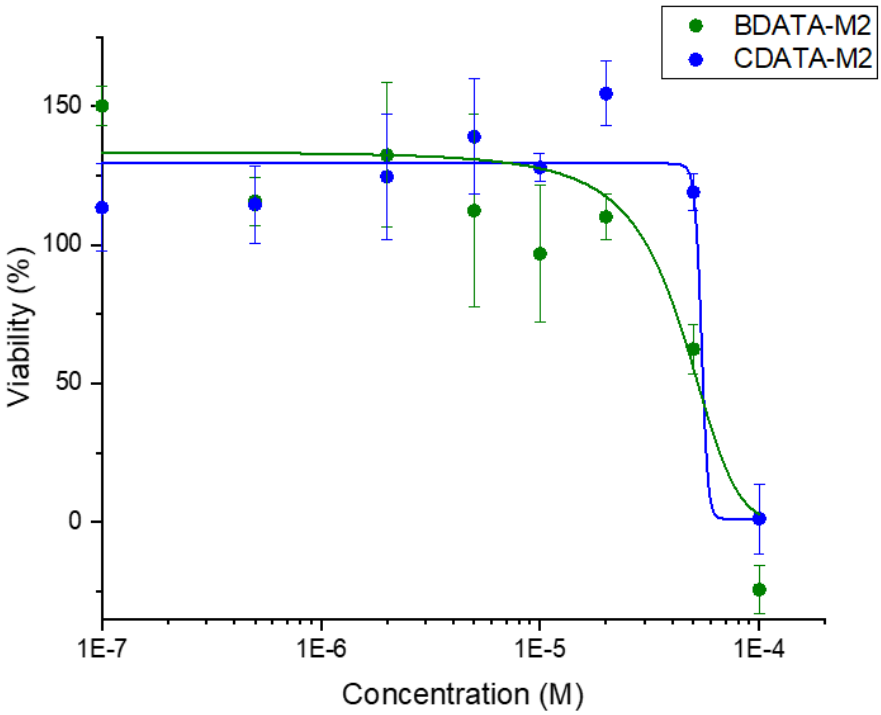

Figure S60. MTS assay of U2OS cells incubated with varying concentrations of **BDATA-M2** and **CDATA-M2**. Data plotted is average of three technical replicates and error bar indicates standard deviation. DMSO-only treated cells defined as 100% viability and wells containing no cells defined as 0% viability. Data fit with DoseResp model using OriginPro. IC50 determined by fit is 44 µM for **BDATA-M2** and 55 µM for **CDATA-M2**.

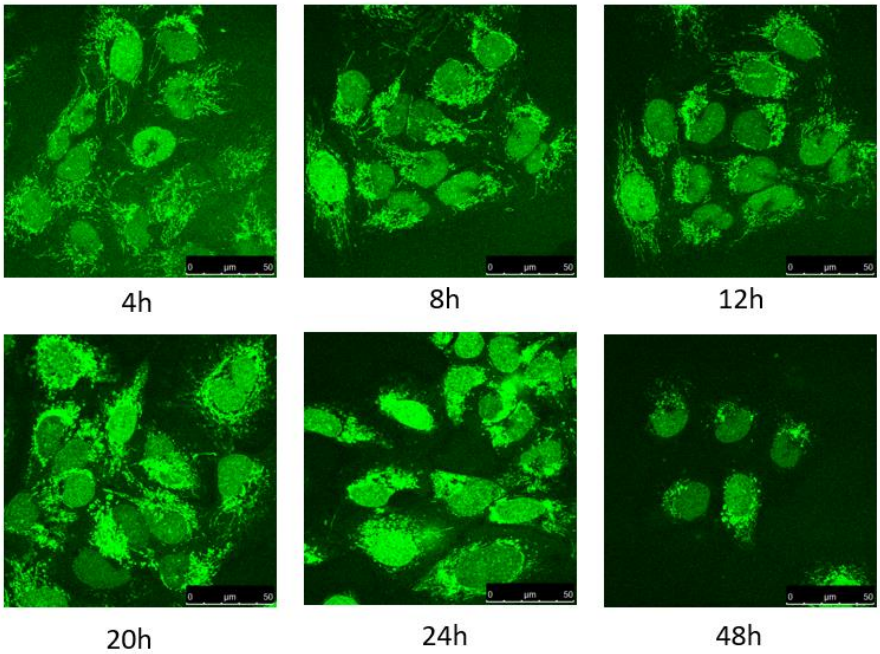

Figure S61. Representative images of U2OS cells incubated with **BDATA-M2** (10 µM) for different incubation times (4-48 h) showing similar localization at each time point.

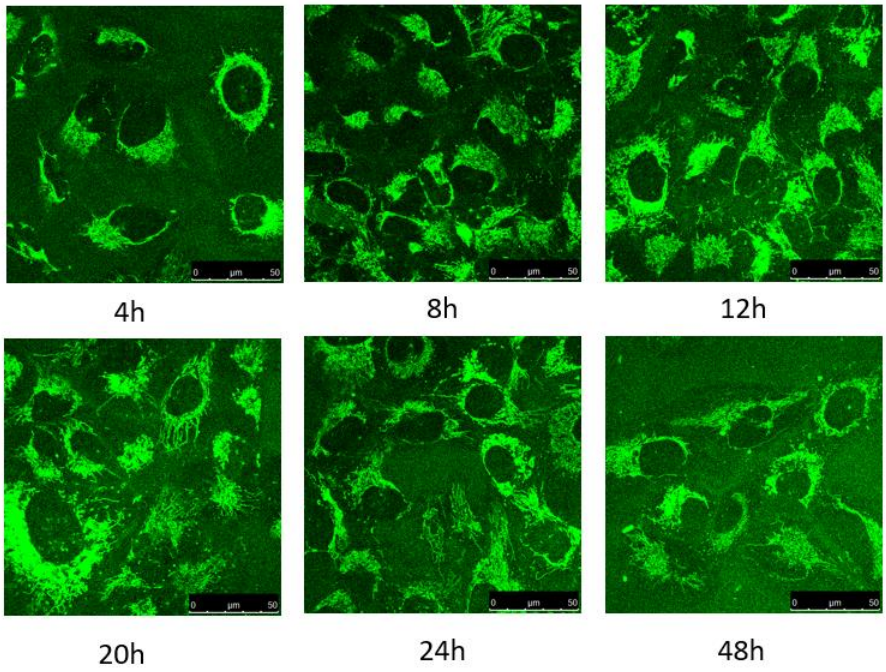

Figure S62. Representative images of U2OS cells incubated with **CDATA-M2** (10 µM) for different incubation times (4-48 h) showing similar localization at each time point.

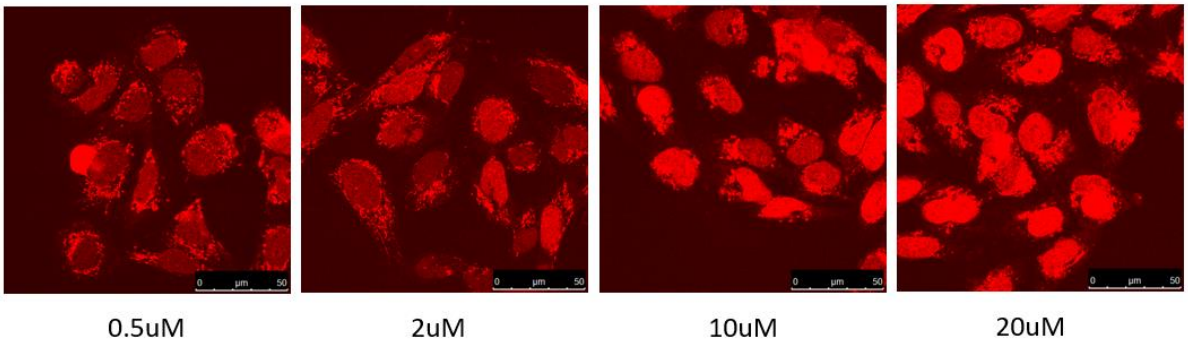

Figure S63. Representative images of U2OS cells incubated with **BDATA-M2** for 24h at different concentrations (0.5-20 µM) showing similar localization at each time point.

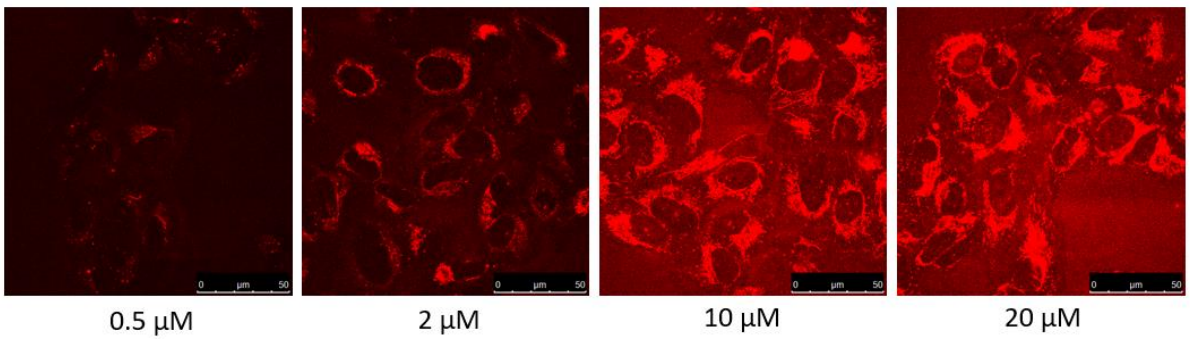

Figure S64. Representative images of U2OS cells incubated with **CDATA-M2** for 24h at different concentrations (0.5-20 µM) showing increasing intensity, but similar localization at each time point.

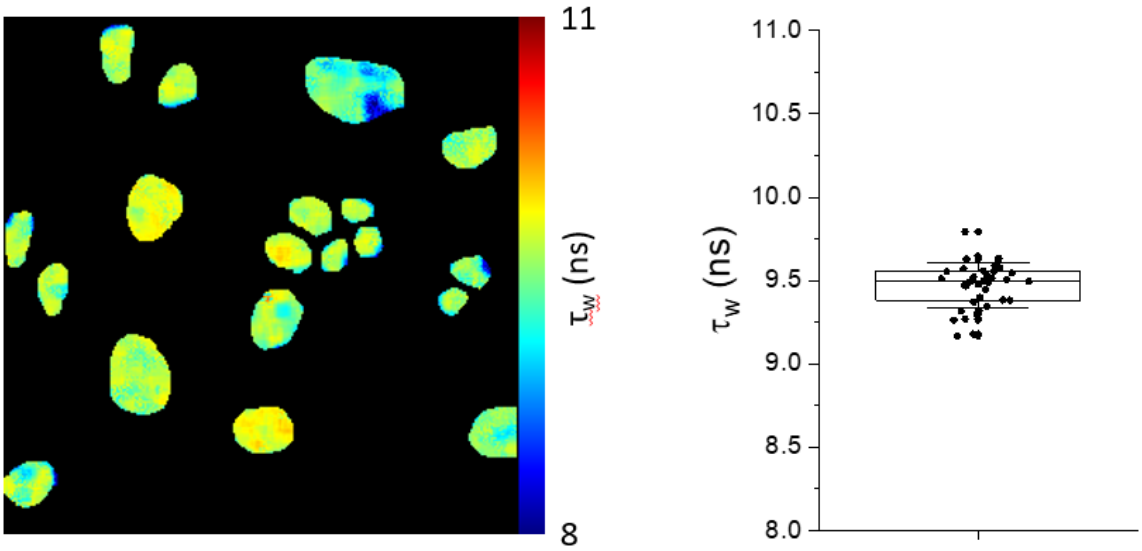

Figure S65. (Left) A representative FLIM image of U2OS cells stained with **BDATA-M2** (10 µM, 24 h) with pixels coloured by intensity-weighted average lifetime. (Right) Box plot of intensity-weighted average lifetime of U2OS cells stained with **BDATA-M2** from four images. Box shows median and interquartile range, bars show one standard deviation, average lifetime observed in individual cell nuclei are overlaid as data points (N = 39).

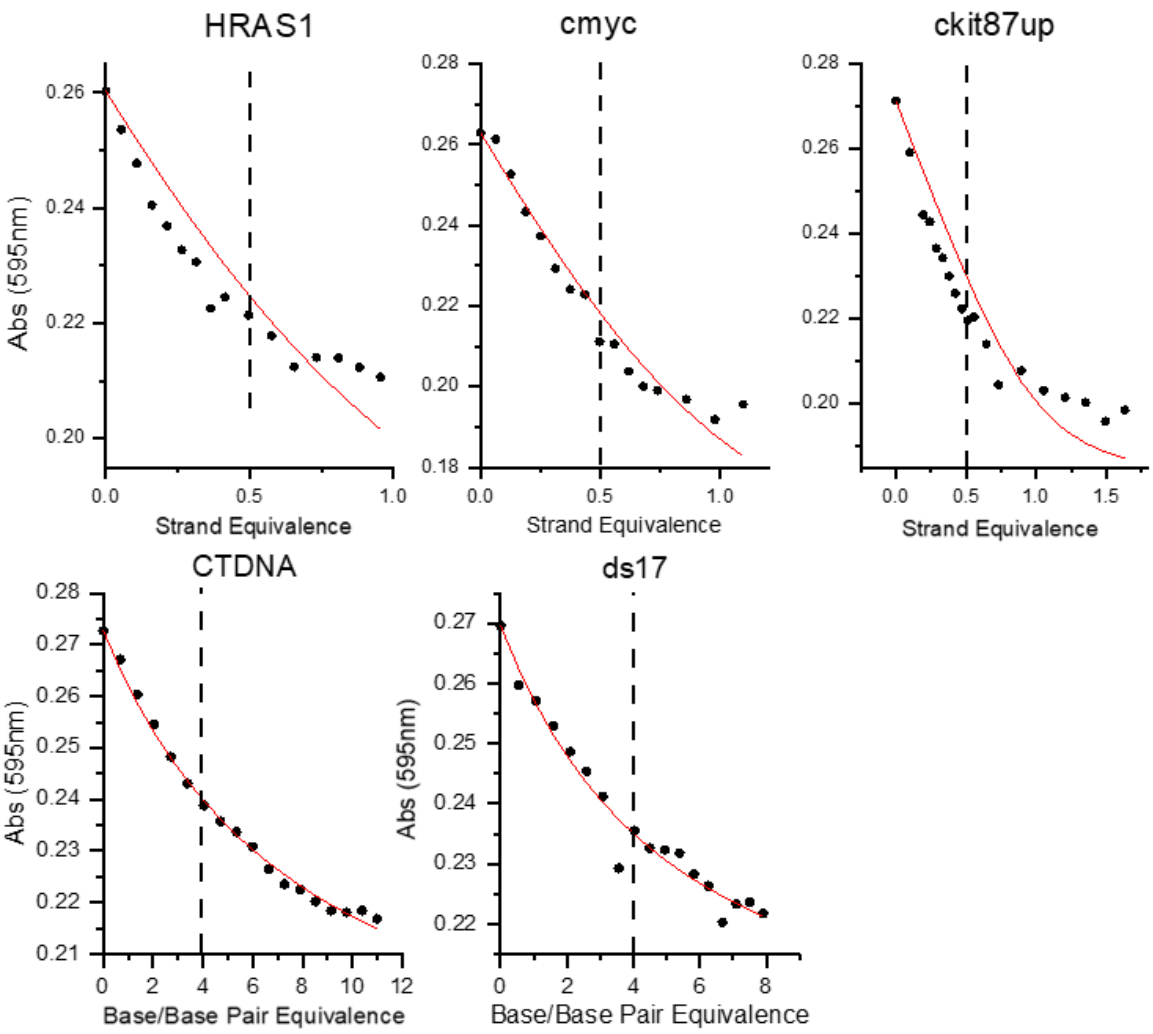

Figure S66. Absorption titrations for **CDATA-M2** with G4 (top) and non-G4 (bottom) forming oligonucleotides or DNA fit to determine binding affinity. The red line shows the fitted binding curve.

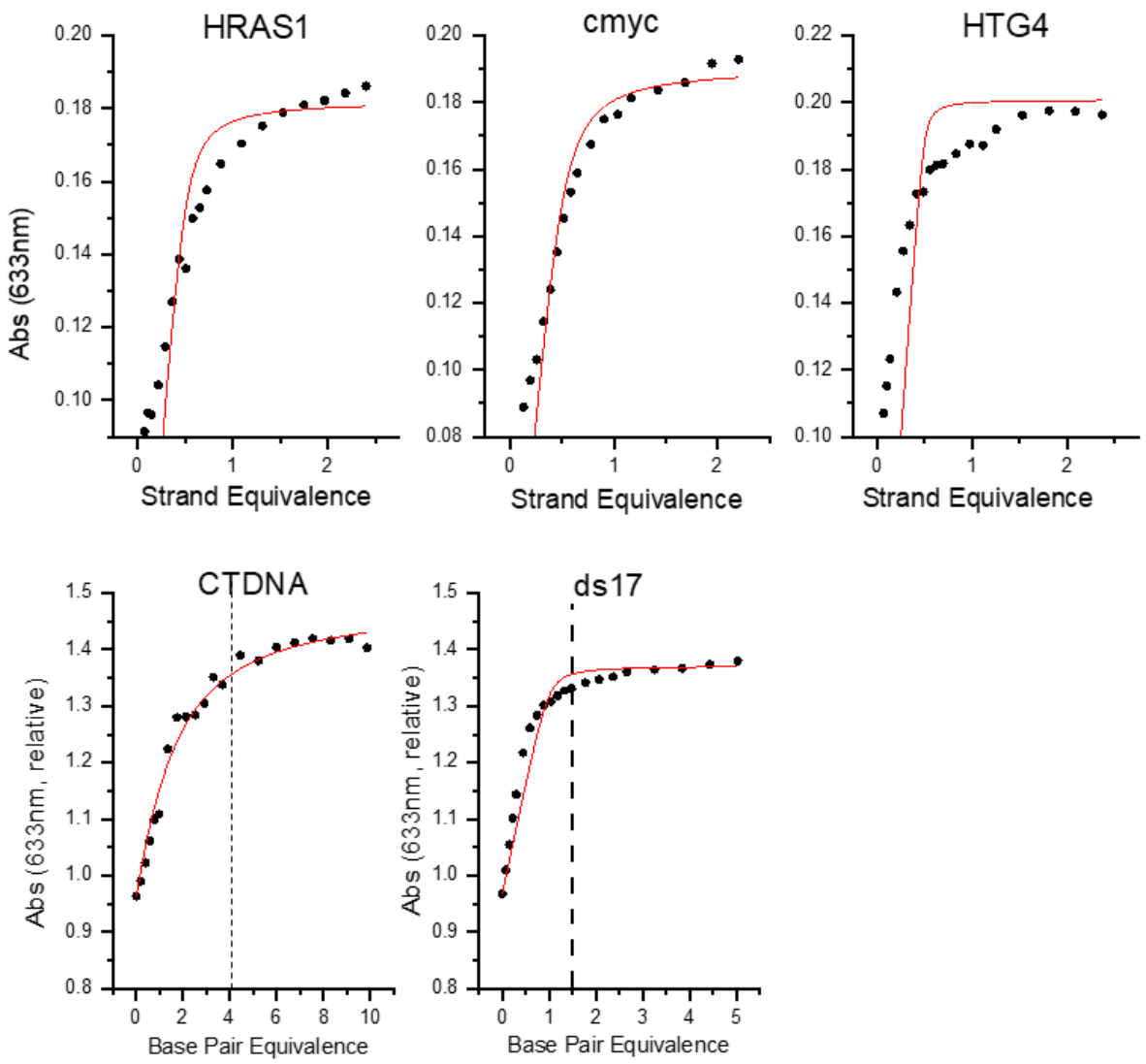

Figure S67. Absorption titrations for **CDATA-M2** with G4 (top) and non-G4 (bottom) forming oligonucleotides or DNA fit to determine binding affinity. The red line shows the fitted binding curve.

Table S4: Binding affinities of **CDATA-M2** and **BDATA-M2** as determined by absorption titrations.

Oligonucleotide	**CDATA-M2 K_a ($x10^5$ M^{-1})**	**Oligonucleotide**	**BDATA-M2 K_a ($x10^5$ M^{-1})**
c-myc	1.2	c-myc	19
ckit87up	3.5	HTG4	230
HRAS-1	0.6	HRAS-1	33
CT-DNA	0.3	CT-DNA	2.5
ds17	0.5	ds17	41

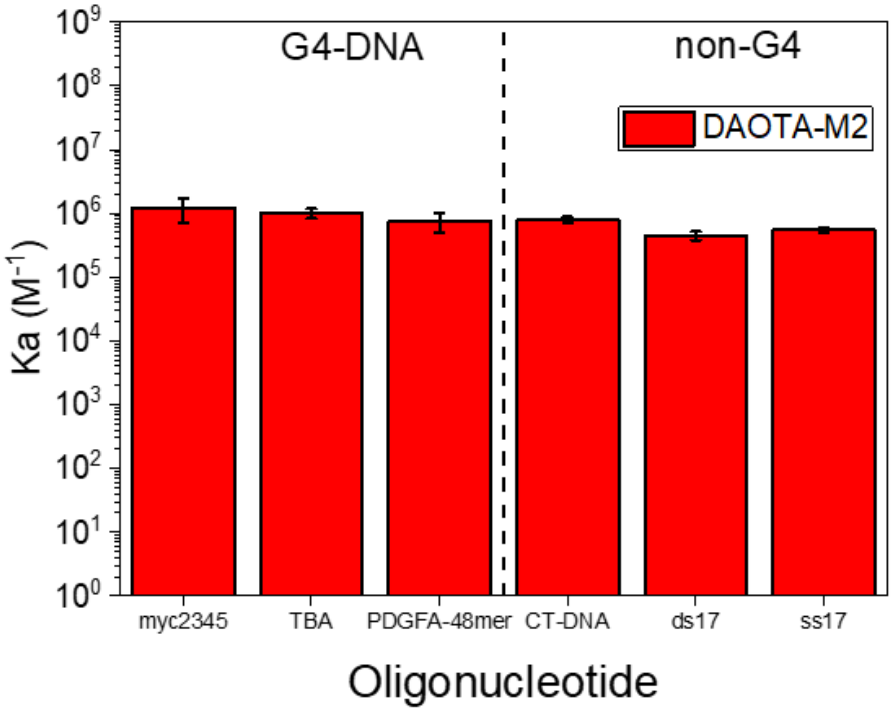

Figure S68. Binding affinities for **DAOTA-M2** bound to a series of G4-forming and non G4-forming oligonucleotides and DNAs. Data within this figure taken from Shivalingam *et.al.*, Nature Communications (2015).